

Neuro Symbolic Knowledge Reasoning for Procedural Video Question Answering with Knowledge Module Learning

Thanh-Son Nguyen^{1,2}, Hong Yang^{1,2}, Tzeh Yuan Neoh^{1,2}, Hao Zhang^{1,2}, Ee Yeo Keat^{1,2}, and Basura Fernando^{1,2,3}

¹ Institute of High-Performance Computing, Agency for Science, Technology and Research, Singapore

² Centre for Frontier AI Research, Agency for Science, Technology and Research, Singapore

³College of Computing and Data Science, Nanyang Technological University, Singapore

Abstract

We introduce PKR-QA (*Procedural Knowledge Reasoning Question Answering*), a new benchmark for question answering over procedural tasks that require structured reasoning. PKR-QA is constructed semi-automatically using a *procedural knowledge graph* (PKG), which encodes task-specific knowledge across diverse domains. The PKG is built by curating and linking information from the COIN instructional video dataset and the ontology, enriched with commonsense knowledge from ConceptNet and structured outputs from Large Language Models (LLMs), followed by manual verification. To generate question-answer pairs, we design graph traversal templates where each template is applied systematically over PKG. To enable interpretable reasoning, we propose a neurosymbolic approach called *Knowledge Module Learning* (KML), which learns procedural relations via neural modules and composes them for structured reasoning with LLMs. Experiments demonstrate that this paradigm improves reasoning performance on PKR-QA and enables step-by-step reasoning traces that facilitate interpretability. Our theoretical analysis on KML learning shows that our trained models satisfy near optimal conditions for learning KG relations as neural network mapping models. Code and dataset will be released soon.

1 Introduction

Interest in understanding procedural tasks is growing, driven by applications in cooking, machinery repair, medical procedures, and daily activities [4, 66, 35], as reflected by platforms like [WikiHow](#). Such tasks consist of sequences of steps, where each step serves a specific purpose and tools are used accordingly. Human understanding of these tasks arises from lifelong learning [49], enriched by commonsense knowledge of objects and their affordances, as well as the ability to reason about temporal and causal dependencies within multi-step processes. This enables individuals to infer not just what to do, but why and how each step contributes to the overarching goal. Emulating this procedural knowledge reasoning—a key aspect of human cognition—is essential for machines to assist in complex real-world tasks.

Despite the rise of visual question answering and general knowledge-based benchmarks, there remains a gap in evaluating a model’s ability to perform procedural knowledge reasoning. To address this, we introduce PKR-QA (*Procedural Knowledge Reasoning Question Answering*), a new benchmark designed to assess Vision Language Models (VLMs) and Neurosymbolic (NS) methods on diverse procedural reasoning capabilities, including multi-hop, deductive, probabilistic, contextual, causal, and counterfactual reasoning. Many procedural tasks require domain-specific knowledge and an understanding of task structures, which can be effectively captured

using knowledge graphs. To construct the PKR-QA questions and answers, we build a *procedural knowledge graph* (PKG) that encodes temporal relationships and causal links among key concepts. Our dataset challenges models to answer procedural questions by combining information from the video with external knowledge about the task. Unlike previous video QA benchmarks that primarily test visual comprehension, i.e., reasoning over what is in the video, our dataset emphasizes task-centric reasoning and knowledge grounded in the procedure. This introduces new challenges that not only demands visual understanding and reasoning, but also to reason about the procedural knowledge of the task [54, 62, 25, 56, 50].

While VLMs demonstrate impressive reasoning and knowledge capabilities, their internal reasoning mechanism is not that transparent. Techniques like chain-of-thought, graph-of-thought, and tree-of-thought aim to enhance VLM reasoning [53, 6, 58], yet the reasoning remains implicit due to the lack of constraints on intermediate variables. Moreover, reasoning and execution are often entangled within the VLM’s internal mechanism. To address this, methods like ViperGPT [47] decouple reasoning from execution by generating executable programs. Inspired by such approaches and neurosymbolic (NS) models [22, 32, 3, 38, 18, 19, 10, 12], we propose Knowledge Module Learning (KML), which models knowledge-based relations as parameterized, trainable modules leveraging on the modern embeddings. KML generate the program of knowledge modules to answer knowledge-based reasoning questions as compositions of knowledge modules using the PKG schema and LLMs. KML explicitly answer knowledge-based reasoning questions leveraging the powerful reasoning mechanism of moderns LLMs allowing it to execute reasoning steps in a more transparent manner to derive the answer. KML supports explicit knowledge-based reasoning, constrained to a well-defined set of knowledge operations, plays a crucial role beyond procedural tasks in domains that require structured decision-making, reliability, and interpretability. KML provides explicit reasoning steps that can be systematically verified, debugged, and refined. Unlike end-to-end black-box models, which often lack transparency in their decision-making, structured reasoning through predefined operations enables more interpretable, trustworthy, and controllable AI systems. Our dataset and the approach promote these aspects.

Our contributions are three-fold. First, we introduce PKR-QA, a new benchmark to test procedural knowledge reasoning by question answering. Second, we propose KML, a neuro-symbolic method that executes LLM-generated programs over knowledge graphs using relation-specific neural modules. Third, we benchmark PKR-QA with state-of-the-art VLMs and NS methods. KML variants outperform all baselines, highlighting the benefit of structured knowledge for interpretable and controllable procedural reasoning. We believe PKR-QA will serve as a valuable resource to advance trustworthy AI in this emerging domain.

2 Related Work

Understanding procedural and instructional videos remains a significant challenge in computer vision, as explored in prior research [33, 4, 66, 64, 35, 8, 45]. The authors in [4] introduced the key step recognition and procedure-aware video representation learning approach using step transitions is presented in [66]. We leverage on these works.

Knowledge-based Visual Question Answering has become popular in recent years [31, 9, 36, 42]. The majority of the past benchmarks on knowledge-based visual question answering are for images while more recently authors in [50] presented a benchmark to evaluate situated and open-world common-sense reasoning in videos with compositionality, temporality, and causality. While the motivation of our work shares similarities with [50], there are notable distinctions. Their focus lies in situated commonsense reasoning grounded in the specific contexts depicted in videos, whereas we concentrate on testing the procedural understanding of models given some partial information such as a step of a task.

Integrating External Knowledge with Video Understanding has been explored

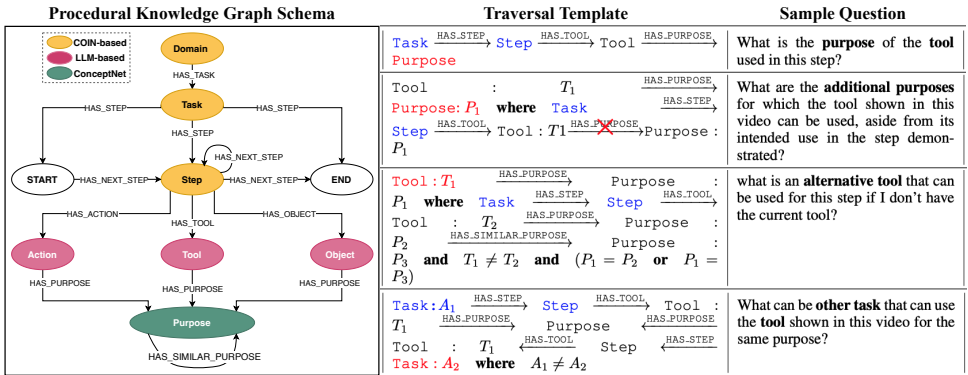


Figure 1: (Left) Schema of the Procedural Knowledge Graph (PKG) showing the high-level abstraction of PKG. In the middle are examples of Traversal Templates that define reasoning patterns over PKG to generate question-answer pairs. Corresponding example questions are shown on the right. In the traversal templates, **blue text** indicates information grounded in the input video, while **red text** denotes the target answer node.

through knowledge graphs (KGs) for tasks like activity recognition [29, 14] and visual commonsense reasoning [26]. VidSitu [41] links events to semantic roles, while TVQA+[23] uses script knowledge for story-based QA. However, these works focus on descriptive reasoning rather than procedural reasoning.

Large VLMs (e.g., Flamingo [2], Video-ChatGPT [30]) and **neurosymbolic** frameworks like ViperGPT [47], MoreVqa [34] and [11] decouple reasoning (e.g., program generation) from execution (e.g., API calls). While ViperGPT uses predefined functions for visual queries, it lacks mechanisms to learn domain-specific knowledge modules or constrain reasoning to procedural logic. Similarly, chain-of-thought prompting [53] improves transparency in LLMs/VLMs but remains dependent on the model’s internal knowledge, which may be unreliable for specialized domains. Our framework advances this by (1) training lightweight, interpretable Knowledge Modules directly from a domain specific KG and (2) constraining reasoning to predefined operations ensuring alignment with domain knowledge.

Our work is also related to NLP research such as [1, 57, 65, 43], which employ **logical queries** to extract information from a KG. This emphasis on curated, domain-specific knowledge is especially valuable for AI assistants operating in contexts where domain expertise, rather than general commonsense reasoning, is crucial for success. Prior knowledge completion works that learns embeddings of entities and relations in KGs are also related to us [7, 52]. In contrast, KML leverage on modern embeddings to learn relational mappings as neural functions, and therefore fundamentally different.

3 PKG Construction and Dataset Creation

Motivated by recent advances in the semi-automated construction of knowledge-based question answering datasets [16], we introduce the *Procedural Knowledge Reasoning Question Answering* (PKR-QA) dataset. It is built on a *Procedural Knowledge Graph* (PKG) that integrates information from the COIN training set, the COIN ontology, GPT-4o-generated annotations, and external commonsense knowledge from ConceptNet, followed by human verification. To enable systematic QA generation, we define a set of question templates and associated Cypher queries [13], which are executed over the knowledge graph to retrieve correct answers. In the following sections, we detail the construction of both the knowledge graph and the QA dataset.

3.0.1 Defining PKG’s Schema (PKGS).

A knowledge graph schema provides a high-level abstraction of the graph, specifying the types of entities that exist and the valid relationships that can occur between them. It serves as a blueprint for structuring the data and interpreting the semantics of the graph. In our case, PKGS contains nodes where each node correspond to a entity type (\mathcal{E}) and edges represent relation types (\mathcal{R}) (Figure 1). The core entity types in PKGS include *Domain*, *Task*, *Step*, *Action*, *Object*, *Tool*, and *Purpose*. Relation types capture meaningful procedural links, such as task-step associations or tool usage (e.g. `HAS_TOOL`), and may carry attributes like *id*, *type*, or additional semantic metadata.

3.0.2 Populating PKG.

Based on this schema, we instantiate PKG by populating it with specific entity and relation instances. Each entity $e \in \mathcal{E}$ has three main attributes: *type*, *name*, and *id*. Relations $r \in \mathcal{R}$ represent specific connections between entity instances. To construct this graph, we integrate annotations from the COIN dataset [48], fine-grained information extracted using GPT-4o [20], and commonsense knowledge from ConceptNet [44].

COIN-based Data (Domain, Task, Step): We extract the procedural structure from the training split of the COIN dataset, which provides annotations for domains, tasks, and steps. For each unique instance of these entities, we create corresponding nodes in the graph. We define `HAS_TASK` edges to link each domain to its associated tasks, and `HAS_STEP` edges to connect tasks to their constituent steps. To capture procedural flow, we analyze step sequences from all training videos and construct `HAS_NEXT_STEP` relations that represent the temporal ordering of steps. Additionally, we introduce special `START` and `END` nodes to explicitly mark task boundaries. Each `HAS_NEXT_STEP` edge is annotated with its observed frequency to model empirical transition likelihoods between steps.

LLM-Augmented Data (Action, Object, Tool): To enhance procedural specificity, we use GPT-4o to extract action-object pairs from step descriptions. For instance, the phrase “remove the tire” yields the action “remove” and the object “tire”. Because COIN lacks explicit tool annotations, we further prompt GPT-4o to infer potential tools for each step. The tool lists are manually verified. We standardize terms (e.g., “scissor” \rightarrow “scissors”), consolidate duplicates (e.g., “marker”, “marker pen”), and unify task-specific variants (e.g., “toilet detergent” \rightarrow “detergent”). Some task-sensitive distinctions are preserved (e.g., “filter” \rightarrow “coffee filter”) when relevant to the procedural context.

ConceptNet-based Data (Purpose): In procedural tasks, actions are typically performed—and tools or objects used—with specific purposes. To represent such intent in our graph, we incorporate commonsense knowledge from ConceptNet, a large-scale semantic network that connects words and phrases through meaningful, human-readable relations such as `UsedFor`, `CapableOf`, and `IsA`. Specifically, we extract potential purposes of actions, tools, and objects using the `UsedFor` and `CapableOf` relations. To contextualize these purposes within specific procedural steps and tasks, we use GPT-4o to infer task- and step-specific interpretations for each entity’s purpose (see the prompt template in Figure 7, Supplementary). This step ensures that the resulting knowledge is not generic but grounded in the procedural context in which the entity is used.

To reduce redundancy and merge semantically similar purposes, we compute pairwise cosine similarities of Sentence-BERT embeddings [40] and apply a similarity threshold of 0.8, validated through manual inspection. Pairs of highly similar purposes are linked using a `HAS_SIMILAR_PURPOSE` edge. The resulting purpose-augmented graph is stored in Neo4j¹, supporting efficient querying and reasoning via Cypher. All contents are manually verified to ensure

¹<https://neo4j.com/>

the reliability of the KG. The constructed KG contains 2,954 unique entities and 12,484 relations. Detailed distributions of entities and relations are shown in Figure 5 (Supplementary).

PKR-QA is a multiple-choice question answering dataset designed to evaluate reasoning over procedural knowledge in instructional videos. Each instance consists of a video segment, a question, five answer choices, and one correct answer. Unlike traditional video QA datasets that focus on grounding answers directly in the visual content of a single video, PKR-QA emphasizes reasoning over procedural knowledge that extends beyond the given video.

3.0.3 Traversal Templates for Procedural Reasoning

We define questions in PKR-QA based on traversal templates which are specific reasoning patterns over PKG. For instance, the traversal $\text{Step} \xrightarrow{\text{HAS_TOOL}} \text{Tool} \xrightarrow{\text{HAS_PURPOSE}} \text{Purpose}$ corresponds to the question: “What is the purpose of the tool used in this step?”. We design 17 such traversal templates to cover a wide range of procedural reasoning types. For each template, we generate multiple question variants using GPT-4o-mini, followed by manual filtering to ensure quality and clarity. These templates form the backbone for producing diverse yet semantically consistent question-answer instances. Figure 1 presents examples of Traversal Templates alongside their corresponding questions. The complete set of 17 question templates with example questions is provided in Table 5 (Supplementary).

3.0.4 Question and Answer Generation

We generate questions by aligning each video segment with its corresponding **Task** and **Step** nodes in PKG, then apply traversal templates to form questions and retrieve answers. For each question, we sample one correct answer and four distractors. To ensure balanced answer distributions and reduce bias, we apply sampling strategies that equalize the frequency of each answer candidate across correct and incorrect options. Each question is paired with a Cypher query that retrieves supporting facts from PKG. These structured annotations serve as logical forms for KG-based evaluation, model supervision, and reasoning trace analysis.

PKR-QA is designed for scenarios with limited training data but having access to structured knowledge, such as a knowledge graph. We construct a training set of 1,700 samples (100 per traversal template) and a validation set of 850 samples (50 per template). The test set contains 46,921 questions, generated from all video segments in the COIN test split. This setup supports zero- and few-shot generalization.

To assess the quality of our dataset, we evaluate whether a question can be reasonably answered by a human—referred to as *plausibility*. We conducted a case study with eight participants, each answering a subset of 170 questions. For each question, participants were shown a video segment, the question, and five answer options, and were asked to select the correct answer. Each question was independently answered by three participants. A question is considered plausible if at least one participant selected the correct answer. Using this criterion, we found that 92.4% of the questions are plausible. Additionally, random baselines perform at chance level ($\sim 20\%$ accuracy), suggesting low annotation artifacts or answer biases.

4 Knowledge Module Learning

In this section, we introduce our proposed *Knowledge Module Learning* (KML) for procedural knowledge reasoning, which effectively handles uncertain (probabilistic) inputs while producing interpretable reasoning outputs using a small number of trainable parameters. We train a collection of neural networks known as Neural Knowledge Module (**KM**) to represent each binary relation type of PKG. Then given a video and a question, we ask LLM to generate a program consisting of KM invocations to answer the questions. Then we execute those KMs

sequentially with the grounded evidence extracted from the video to obtain the final answer. Next, we present the details.

Knowledge Module Learning. For each binary relation type $\mathcal{R}_k(\mathcal{E}_i, \mathcal{E}_j)$ in the PKG that maps from entity type \mathcal{E}_i to \mathcal{E}_j , we learn a KM as a learnable neural relation $(\phi_{\mathcal{R}_k})$ with parameters $(\theta_{\mathcal{R}_k})$. KM learns to map from a given head entity $e_i \in \mathcal{E}_i$ to the corresponding set of tail entities \mathcal{I}_j where $\mathcal{I}_j \subseteq \mathcal{E}_j$ of relation \mathcal{R}_k as follows:

$$\phi_{\mathcal{R}_k}(x(e_i; \theta_x); \theta_{\mathcal{R}_k}) \rightarrow \mathbf{e}_j \quad (1)$$

where $x(e_i; \theta_x)$ is a d-dimensional embeddings of the head entity and \mathbf{e}_j is a vector that is closer to $x(e_j)$ for all $e_j \in \mathcal{I}_j$. Here, \mathcal{I}_j is the set of tail entities under relation R_k for the head entity e_i or formally $\mathcal{I}_j := \{e_j \in \mathcal{E} \mid R_k(e_i, e_j) = \text{True}\}$. Then the objective of KM learning is to make sure to learn $(\theta_{\mathcal{R}_k}, \theta_x)$ such that for each head entity embedding $x(e_i)$ can be mapped to a vector \mathbf{e}_j that is representative of all corresponding tail entities \mathcal{I}_j . We iterate over all the triplets (including the inverse triplets) of all relation types of PKG in a batch-learning manner and train the KMs using the contrastive loss.

$$-\log \frac{\exp(\frac{\mathbf{e}_j \cdot x(e_j)}{\tau})}{\sum_{\forall e_p \in \mathcal{B}} \exp(\frac{\mathbf{e}_j \cdot x(e_p)}{\tau})} \quad (2)$$

Here \mathcal{B} is the set of tail entities in the batch of triplets excluding \mathcal{I}_j , $e_j \in \mathcal{I}_j$ is one of the positive target entity for e_i under R_k , and τ is the temperature. Note that we L2 normalize all embeddings and the vector \mathbf{e}_j before computing the contrastive loss. Contrastive loss plays a crucial role in learning neural relation functions $\phi_{\mathcal{R}_k}$ (i.e. KMs), for modelling symbolic binary relations of the form $\mathcal{R}_k(\mathcal{E}_i, \mathcal{E}_j)$.

The embedding learning function $x(\cdot; \theta_x)$ is implemented using CLIP [39] text encoder embeddings with frozen parameters (θ_x) . Alternatively, we also learn the embedding function from scratch using standard implementations². Similarly, we also learn the inverse KM for each inverse relation $\mathcal{R}_k^*(\mathcal{E}_j, \mathcal{E}_i)$ of each relation \mathcal{R}_k . Let us denote the set of all KMs by $\phi_{\mathcal{R}} = \{\phi_{\mathcal{R}_k} \mid k = 1, \dots\}$.

At inference, KM takes an input embedding and maps that to an output embedding that represents a set of corresponding tail entities of that relation. For example, Table 3 shows the semantic meaning of each output embedding that maps to a set of tail entities of relation HAS_TOOL for given input embedding of the Step entity. We experimented with different neural configurations of multi-layered perceptron (MLP) and found that two-layered MLP with *Tanh* activation performs the best for learning KMs. Next, we present how to answer questions using KMs and LLM generated programs.

Question Answering. Given the video v , the question Q , and options $Y = \{y_1, \dots, y_n\}$ ($n = 5$) we prompt a LLM $\phi()$ to find the relevant entity type (E_g) that should be grounded in the video to answer the question.

$$\phi(Q, \text{PKGS}) \rightarrow E_g \quad (3)$$

For example, E_g can be a task, step, object or action. Then we find the entity instance(s) that is present in the given video V of the entity type E_g using a vision foundation model (VLM) as follows:

$$\text{VLM}(V, E_g) \rightarrow \mathbf{x}_e \quad (4)$$

where $\mathbf{x}_e \in \mathcal{R}^C$ represents the score vector for the entity type (e.g., step distribution) across all categories of that entity type. We assume there are C categories for entity type E_g . To obtain

²We learn these using `torch.nn.Embedding`

estimates about the grounding entity E_g , we use *ProceduralVRL* (P.VRL) [64] a VLM tailored for procedural tasks.

Given the collection of Knowledge Module names (ϕ_R) and the question Q , and the grounded entity type E_g , we use LLM (denoted by $\phi_G()$) to generate a list of sequence of Knowledge module invocations (known as program or P_1) to answer the question. Using a similar concept to chain-of-thought [53, 51], tree-of-thought [58], and graph-of-thought [6] we ask the LLM to generate multiple alternative programs to answer the same questions.

$$\begin{aligned}\phi_G(Q, \phi_R, E_g) = [P_1 = \langle \phi_{r_i}, \phi_{r_j}, \phi_{r_k}, \dots \rangle, \dots, \\ P_l = \langle \phi_{r_i}, \phi_{r_j}, \phi_{r_k}, \dots \rangle]\end{aligned}\quad (5)$$

Here P_l is the specific module invocations and each P_l may result in different answers following an alternative-thought of reasoning approach. The LLM module $\phi_G()$ can be implemented with any LLM with good reasoning capability. We use a special prompt that invokes deep understanding and consistent knowledge graph traversal and alternative thought invocations— see supplementary material for more details on the prompt. As an example, to answer the question **what is an alternative tool that can be used for this step?** it generates the following program of modules.

HAS_TOOL(Step) → Tool
 HAS_PURPOSE(Tool) → Purpose
 SIMILAR_PURPOSE(Purpose) → Purpose
 PURPOSE_TO_TOOL(Purpose) → Tool

where PURPOSE_TO_TOOL(Purpose) is the inverse relation of HAS_PURPOSE(Tool). LLM may generate multiple programs that leads to the answer, typically 3-5 alternatives for complex problems. To predict the answer, we execute each program in order, inputting the grounded entity representation z_i into the first module. For each program (P_1 to P_l), z_i is fed into the first module to obtain intermediate embedding, invoking all modules sequentially. For example $z_j = \phi_{r_i}(z_i)$ then $z_k = \phi_{r_j}(z_j)$ and finally $z_f = \phi_{r_k}(z_k)$. Therefore the *final embedding* representing the answer to the given question is z_f . We can also inspect the meaning of each intermediate representation as shown in Table 3 allowing more interpretable reasoning that can handle uncertain inputs.

To compute the first input embedding z_i , we use the grounded top-K entity instance and weight the embeddings of each grounded entity instance category name as follows:

$$z_i = S \times \mathbf{X}_e^T \quad (6)$$

$$\mathbf{X}_e = [x(e_1), x(e_2), \dots, x(e_k)] \quad (7)$$

where e_k is the k -th category of the entity type E_g and $S = [s_1, s_2, \dots, s_k]$ is a vector containing top-k scores for each grounded entity-type category (e.g. Step categories).

Inference Given the options $Y = \{y_1, \dots, y_n\}$, we obtain the embeddings of Y , i.e., $x(Y) = [x(y_1), x(y_2), \dots, x(y_n)]$. Then we compute the cosine similarity between the *final embedding* z_f and $x(Y)$ and apply softmax to predict the answer index for each program. When there are alternative programs, we take the maximum score from all programs as the final answer.

VQA Training for KML. We also fine-tune the KMs using a few examples of the video-question-answer using our dataset. We compute the cosine similarity between z_f and $x(Y)$ and apply softmax to predict the answer index.

$$\hat{y} = \text{softmax}(\text{cosine_sim}(x(Y), z_f)) \quad (8)$$

Then we train all KMs jointly using the cross-entropy loss over the correct answer index. At test time, we predict the right answer using the argmax of the cosine similarity scores. One of the advantages of KML (auto-program) approach is that, given the relation types, we do not need to manually select any neural modules, or generate programs manually. We use LLMs such as GPT, DeepSeek or Mistral. More implementation details of KML is presented in the supplementary.

5 Experiments

5.1 Experimental Setup

We conduct experiments on the PKR-QA benchmark to evaluate the effectiveness of VLMs and Neurosymbolic methods for procedural knowledge-based question answering. We use NVIDIA A100 GPUs (80GB VRAM) for conducting experiments with VLMs, NVIDIA GeForce RTX 2080 Ti and A5000 GPUs (60GB VRAM) for training KML, and RTX 3090 GPUs (24GB VRAM) for training knowledge graph embedding methods.

VLM Evaluation Settings. We evaluate VLMs under five different settings to assess their procedural knowledge reasoning ability: (1) **Zero-shot**: VLMs take a video segment (8 uniformly sampled frames), a question, and options as input; (2) **VLM+P.VRL**: VLMs take a video segment (8 uniformly sampled frames), a question, options, and the top-5 step/task categories from P.VRL as input; (3) **KG-training**: VLMs are tuned using the triplet instances of our PKG as questions using LoRA [17] and then evaluate the fine-tuned VLMs with PKR-QA; (4) **QA training**: VLMs are tuned using LoRA for 100 epochs with 4 randomly sampled frames as input, demonstrating the impact of few-shot fine-tuning. All models are trained using the training set of 1,700 question-answer pairs; (5) **KG+QA training**: VLMs are tuned using triplet instances following KG-training, and 1,700 question-answer pairs as described in QA training.

Neurosymbolic Methods. We explore three variants of KML, differing in how the embedding function $x(\cdot; \theta_x)$ is implemented. In **KML-F-CLIP**, $x(\cdot; \theta_x)$ is a frozen CLIP text encoder. In **KML-CLIP**, we initialize $x(\cdot; \theta_x)$ with CLIP embeddings and fine-tune its parameters. In **KML-Rand**, θ_x is learned from scratch (i.e., randomly initialized). We compare our KML against the following NS methods:

Inference by Graph Propagation (IGP): We implement a simple NS baseline that uses a given program and a set of grounded entities with associated probabilities or logits to answer questions. Given a directed knowledge graph with binary relations, we propagate uncertainty from grounded entities through the relations specified in the program. Using breadth-first traversal, we accumulate scores at each target entity by summing the propagated logits. This approach resembles probabilistic logic-based inference.

KG Embedding Methods: We compare against standard KG embedding models, including TransE [7], TransH [52], and RotatE [46]. After training, we use LLM-generated programs (as in KML) to perform multi-hop reasoning. These models are selected for their support of compositional reasoning. Embedding dimensions are tuned on a validation set, yielding optimal sizes of 256 for TransE, 100 for TransH, and 256 for RotatE. We also include variants with CLIP-initialized entity and relation embeddings to enable direct comparison with CLIP-based KML models.

Modern NS methods: We compare with modern NS methods including ViperGPT [47] that uses the power of LLM and vision models, and MAC [19]. We evaluate MAC on a classification-based VQA task, using a single image frame and a question (without answer choices) as input. The model predicts from 2,079 answer classes aggregated from the dataset. We use GloVe [37] embeddings for text and extract visual features with a pretrained ResNet101 [15]. We tuned the embedding size, MAC hidden size, and the number of MAC layers, selecting the best setup based on validation performance.

Metrics. Since VLM-generated text may not exactly match the predefined multiple-choice options, we adopt the filtering and MCQ accuracy computation strategy from [63, 27]. We report both overall accuracy and mean accuracy for each model. **Accuracy** is computed as

Setting	Model	Acc	mAcc
Zero-shot	DeepSeek-VL2 (27.4B) [55]	58.4	55.4
	MiniCPM-V (8B) [59]	62.6	59.7
	mPLUG-Owl3 (7B) [60]	<u>63.1</u>	<u>60.2</u>
	Qwen2.5-VL (7B) [5]	59.6	57.8
	VideoChat2-HD (7B) [24]	61.2	58.4
VLM + P.VRL	DeepSeek-VL2 (27.4B) [55]	64.5	59.9
	MiniCPM-V (8B) [59]	67.4	63.8
	mPLUG-Owl3 (7B) [60]	65.5	61.6
	Qwen2.5-VL (7B) [5]	<u>69.4</u>	<u>65.8</u>
	VideoChat2-HD (7B) [24]	65.5	59.9
KG-training	MiniCPM-V (8B) [59]	63.5	61.0
	mPLUG-Owl3 (7B) [60]	64.8	61.4
	Qwen2.5-VL (7B) [5]	<u>67.3</u>	<u>64.1</u>
QA training	MiniCPM-V (8B) [59]	71.1	71.4
	mPLUG-Owl3 (7B) [60]	71.8	72.4
	Qwen2.5-VL (7B) [5]	<u>73.6</u>	<u>73.4</u>
KG+QA training	MiniCPM-V (8B) [59]	72.1	72.1
	mPLUG-Owl3 (7B) [60]	73.1	73.8
	Qwen2.5-VL (7B) [5]	74.2	73.8

Table 1: Comparison of VLMs in different settings. Underlined scores denote the best-performing method within each setting, while bold scores highlight the best overall.

the average score across all test samples, while **mean accuracy** (mAcc) is the average of per-template accuracies, providing equal weight to each traversal template.

5.2 Analysis and Discussion

Benchmarking VLMs on PKR-QA. Table 1 compares the performance of various VLMs across five training and inference settings, revealing several key insights. **Providing predicted step and task** information from ProceduralVRL (VLM+P.VRL) consistently improves performance over the **zero-shot** setting. These gains highlight the importance of grounded procedural context in enhancing reasoning, even for strong models like MiniCPM-V and Qwen2.5-VL. **Training on KG triplets** yields some improvement over zero-shot baselines, though the gains are modest and less consistent, suggesting that aligning symbolic representations with multimodal inputs remains non-trivial. **QA-based fine-tuning** leads to larger improvements, particularly for MiniCPM-V and Qwen2.5-VL. These gains indicate that VLMs are capable of adapting to task-specific supervision, even when provided with a relatively small number of QA pairs (1,700 samples). The best performance is achieved when **combining both KG and QA training**, with Qwen2.5-VL reaching 74.2/73.8, indicating that integrating structured procedural knowledge with task-specific examples provides complementary benefits for enhancing procedural understanding in VLMs.

Benchmarking Neurosymbolic Methods. As shown in Table 2, all KML variants outperform all baselines, demonstrating the benefit of executing LLM-generated KG traversal programs with relation-specific KM for the proposed procedural reasoning question answering task. KML achieves the highest performance under KG+QA training using KML-CLIP variant. The performance of KML-Rand is not far from KML-F-CLIP and interestingly, when

Setting	Model	Acc	mAcc
No Training / No Program	ViperGPT	41.6	40.9
	GPT-4o + P.VRL	<u>71.2</u>	<u>69.0</u>
Program Only	IGP (+P.VRL)	62.8	60.0
QA training Only	MAC	11.6	20.0
KG-training	TransE	63.6	51.6
	TransH	<u>73.1</u>	66.3
	RotatE	41.6	29.2
	TransE+CLIP	56.8	45.4
	TransH+CLIP	70.6	65.9
	RotatE+CLIP	48.8	35.2
	KML-F-CLIP (Ours)	74.6	<u>71.6</u>
	KML-Rand (Ours)	<u>73.5</u>	70.0
	KML-CLIP (Ours)	<u>75.3</u>	71.5
KG+QA training	KML-F-CLIP (Ours)	76.7	75.3
	KML-Rand (Ours)	<u>77.4</u>	76.3
	KML-CLIP (Ours)	78.1	77.1

Table 2: Performance comparison of NS methods.

tuned with KG+QA training the KML-Rand performs better than KML-F-CLIP under the same setting. **ViperGPT** performs poorly on our benchmark due to the absence of built-in reasoning operators and reliance on predefined program templates that are not suited for the structured reasoning required in procedural knowledge tasks. **IGP** suffers from combinatorial explosion and poor grounding, often generating irrelevant results from uncertain starting nodes. In contrast, KML handles such uncertainty better by grounding traversal via learned knowledge modules. **MAC**, originally designed for visual reasoning tasks (e.g., answering questions like “What is to the left of the green box?”), fails in our setting due to its lack of access to external procedural knowledge. Among **KG embedding methods**, TransE and TransH perform better due to their additive or projective composition, aligning well with our program-based reasoning. RotatE underperforms, likely because its complex-valued, rotation-based composition is less effective for multi-hop reasoning. CLIP-based initialization yields mixed results—improving RotatE but degrading TransE and TransH—indicating varying alignment with visual semantics across models. We also evaluate **GPT-4o** using top-5 predicted step/task category names from P.VRL. It achieves 71.2% accuracy and 69.0% mean accuracy.

KML’s Interpretability. One key advantage of KML is its interpretability, as illustrated in the qualitative examples in Table 3 and Table 4. We observe step-by-step reasoning and intermediate interpretations from the learned embeddings, offering insight into the model’s decision process. The output entities represented by the output vectors of each KM seems reasonable and accurate for the given task.

	Q. What is the other task that use the tool in this video for the same purpose?	Task: Make Orange Juice Step: pour the orange juice into the cup
HAS_TOOL	TOOL_TO_STEP	STEP_TO_TASK
Out=Tool	Out=Step	Out=Task
cup (0.361) mug (0.273) measuring cup (0.253) yogurt (0.249) bottle (0.223)	pour into the ingredients (0.337) pour in after mix it (0.314) add some ingredients to the tea (0.308) add some ingredients in the coffee (0.307) pour the ingredients into the bowl (0.293)	MakeCookie (0.221) MakeCocktail (0.208) MakeHomemadeIceCream (0.191) MakeChocolate (0.188) MakeCoffee (0.185)

Table 3: Three-hop Reasoning using KML-F-CLIP: The step-by-step reasoning outputs of KML with estimated probability value over the domain of relation using embeddings.

KML’s Generalizability. To assess KML’s generalizability, we added ten binary relations from the **STAR benchmark**. KML-F-CLIP achieved 74.9% on Interaction and 76.7% on Feasibility questions, outperforming prior bests of 71.8% [21] and 62.4% [61]. For Sequence and Prediction questions, it scored 57.3% and 49.8%, respectively. We also trained KML-F-CLIP using a **GPT-4o-generated KG** from 7,687 WikiHow tasks (57,027 steps, 8.7M triplets) capturing tools, actions, objects, and purposes. Evaluated on our PKR-QA dataset, it achieved 73.9% mean accuracy, rising to 74.9% with KG+QA training, suggesting that while generic KGs help, domain-specific modules remain advantageous.

KML’s Robustness. Figure 2 (left) shows KML’s performance using top- k step/task predictions ($k = 1$ to 5). Using all top-5 predictions yields the best QA performance, while top-1 predictions still achieve strong results, demonstrating the model’s robustness to imperfect inputs. Figure 2 (right) reports a moderate correlation (0.24) between step prediction accuracy and QA accuracy, suggesting KML does not heavily depend on input quality, benefiting from embedding-based reasoning and generalizable knowledge modules.

KML Ablation. We train KML modules from scratch using only QA training, with KML-F-CLIP achieving 59.3% mean accuracy—highlighting the value of training on PKG data. KML allows exploration of multiple programs per question (see supplementary), though gains over single-program use are marginal. It also supports expert program editing for improved reliability. Evaluating different LLMs for program generation in KML-F-CLIP, GPT-4o leads with 71.6% accuracy, followed by LLaMA-3-8B (68.4), DeepSeek-V2.5 (66.5), Mistral-7B (66.2), and Qwen-2.5 (63.7), showing KML’s robustness across LLM models.

		<p>Q. What is an alternative tool can be used for this step?</p>	<p>Task: Polish Car Step: clean the scratch</p>
HAS_TOOL	HAS_PURPOSE	SIMILAR_PURPOSE	PURPOSE_TO_TOOL
Out=Tool	Out=Purpose	Out=Purpose	Out=Tool
microfiber towel (0.237)	wiping up dust (0.249)	cleaning things (0.233)	cloth (0.263)
microfiber cloth (0.229)	dusting (0.241)	cleaning (0.219)	towel (0.253)
polishing pad (0.217)	cleaning (0.238)	wiping up wet spill (0.205)	soap (0.219)
cloth (0.168)	wiping up wet spill (0.228)	clean dirty things (0.204)	curtains (0.178)
towel (0.125)	wiping (0.215)	cleaning up (0.200)	cushion (0.178)

Table 4: Four-hop Reasoning using KML-F-CLIP: The step-by-step reasoning outputs of KML with estimated probability value over the domain of relation using embeddings.

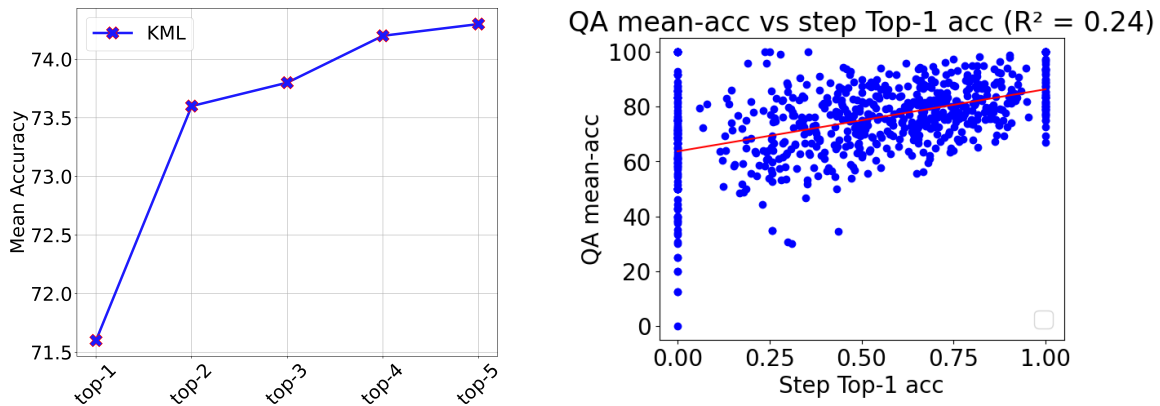


Figure 2: (Left) QA performance of KML-F-CLIP using top-1 to top-5 grounded entities from P.VRL. (Right) Correlation between step prediction accuracy and QA accuracy.

5.3 Theoretical analysis on the KML learning.

The objective of KML is to learn a neural network mapping function

$$\phi_{R_k}(x(e_i; \theta_x); \theta_{R_k}) \rightarrow \mathbf{e}_j$$

where \mathbf{e}_j is a vector that is closer to $x(e_j)$ for all $e_j \in \mathcal{I}_j$.

For this theoretical analysis without loss of generality let us introduce the following problem to study neural mapping such as ϕ_{R_k} .

Let $X = \{x_1, x_2, \dots, x_n\}$ be a finite set of vectors representing the learned embeddings of each entity in the KG. For each $x \in X$ we define:

- $Y(x) \subseteq X$: the set of *positive target entity embeddings* for x under the relation.
- $U(x) := X \setminus Y(x)$: the set of *negatives* entity embeddings under the relation.
- $z = \phi(x)$: the vector mapping of x under the relation.
- Each $z := \frac{z}{\|z\|_2}$: the normalized embedding (unit vector).

Then let us define cosine similarity

$$s(a, b) := \langle a, b \rangle, \quad a, b \in \mathbb{R}^D, \|a\| = \|b\| = 1,$$

so that $s(a, b) \in [-1, 1]$.

Similarity-based constraint for KML optimization

The optimal condition for KML learning is to make sure that

$$\min_{y \in Y(x)} s(\phi(x), y) > \max_{u \in U(x)} s(\phi(x), u). \quad (9)$$

. The cosine-similarity-based constraint requires that the *least similar positive* still has higher cosine similarity (with z) than the *most similar negative*.

Implications for the mapping ϕ

The above constraints imply several structural requirements on ϕ :

- **Unit-normalization:** Outputs must be normalized:

$$\|\phi(x)\|_2 = 1, \quad \forall x \in X.$$

- **Non-collapse:** ϕ must not map all inputs to the same unit vector, otherwise eq. (9) cannot be satisfied.
- **Continuity:** ϕ should be Lipschitz continuous in the angular metric, so that small perturbations in x do not drastically change $\phi(x)$.

Bound on the contrastive loss

We define the multi-positive contrastive loss for KML as follows:

$$\mathcal{L}(x) = -\log \frac{\sum_{y \in Y(x)} \exp(s(\phi(x), y)/\tau)}{\sum_{v \in X} \exp(s(\phi(x), v)/\tau)}, \quad (10)$$

where $\tau > 0$ is a temperature parameter. For simplicity of the proof we drop the temperature.

Let us denote $s_v := s(\phi(x), v)$. Then let us define A, B and C as follows:

$$A = \sum_{y \in Y(x)} e^{s_y}, \quad C = \sum_{u \in U(x)} e^{s_u}, \quad B = A + C,$$

Let us denote ε to be such that $\mathcal{L}(x) \leq \varepsilon$. Then we obtain

$$\frac{A}{A + C} \geq e^{-\varepsilon} \iff C \leq (e^\varepsilon - 1)A. \quad (i)$$

We know that

$$\begin{aligned} \sum_{i=1}^{|Y(x)|} e^{\min_{y \in Y(x)} s_y} &\leq \sum_{y \in Y(x)} e^{s_y} \\ \Rightarrow |Y(x)| e^{\min_{y \in Y(x)} s_y} &\leq A \\ \Rightarrow \min_{y \in Y(x)} s_y &\leq \log(A) - \log(|Y(x)|) \end{aligned} \quad (ii)$$

Similarly,

$$\begin{aligned} \sum_{u \in U(x)} e^{s_u} &\geq e^{\max_{u \in U(x)} s_u} \\ \Rightarrow \max_{u \in U(x)} s_u &\leq \log(C) \end{aligned} \quad (iii)$$

From (i) and (iii)

$$\begin{aligned} \max_{u \in U(x)} s_u &\leq \log((e^\varepsilon - 1)A) \\ \Rightarrow \max_{u \in U(x)} s_u &\leq \log(e^\varepsilon - 1) + \log(A) \end{aligned} \quad (iv)$$

From (ii) - (iv)

$$\begin{aligned} \min_{y \in Y(x)} s_y - \max_{u \in U(x)} s_u &\leq -\log(|Y(x)|) - \log(e^\varepsilon - 1) \\ \Rightarrow \min_{y \in Y(x)} s_y - \max_{u \in U(x)} s_u &\leq \log\left(\frac{1}{|Y(x)|(e^\varepsilon - 1)}\right). \end{aligned}$$

As the left hand size should be > 0 , the $\log\left(\frac{1}{|Y(x)|(e^\varepsilon - 1)}\right)$ can be > 0 iff $\frac{1}{|Y(x)|(e^\varepsilon - 1)} > 1$.

Therefore,

$$\begin{aligned} 1 + Y(x) &> Y(x)e^\varepsilon \\ \Rightarrow \log(1 + Y(x)) - \log(Y(x)) &> \varepsilon \\ \Rightarrow \varepsilon &< \log(1 + Y(x)) - \log(Y(x)) \\ \Rightarrow \varepsilon &< \log\left(1 + \frac{1}{Y(x)}\right) \end{aligned}$$

As $L(x) \leq \varepsilon$, if

$$\mathcal{L}(x) < \log\left(1 + \frac{1}{|Y(x)|}\right), \quad (11)$$

then the right-hand side is positive, which implies

$$\min_{y \in Y(x)} s_y > \max_{u \in U(x)} s_u,$$

and therefore cosine constraint holds.

In our experiments, we obtain a loss of 0.71 which aligns with this bound. The temperature simply rescales the needed loss threshold by τ (larger τ makes the separation easier but gradients smaller). Therefore, τ has to be set depending on the batch size. We set the τ to be batch size.

As our KML neural network can be written as follows:

$$f(x) = h(g(x))$$

where

$$h(x) = \frac{x}{\|x\|}$$

and

$$g(x) = W_1 \tanh(W_2 x).$$

As

$$\|h(u) - h(v)\| \leq \frac{2}{\delta} \|u - v\|$$

and

$$\|g(u) - g(v)\| \leq \|W_1\| \cdot \|W_2\|$$

The Lipschitz constant for our Knowledge Modules is given by

$$L = \frac{2}{\delta} \|W_1\| \cdot \|W_2\|,$$

where δ denotes the minimum norm of $g(x)$ over all x . This implies that, as long as the neural network $g(x)$ does not produce vectors with very small norms, learning can proceed effectively.

In particular, this result shows that our neural networks are Lipschitz continuous whenever $\delta > 0$. It also motivates the use of weight regularization (e.g., weight decay), which we apply with a decay factor of 0.01 during training.

Moreover, this analysis suggests that when learning embeddings, it may be beneficial to use larger embedding dimensions D , as they help avoid excessively small vector norms and thus improve stability. The choice of $W_1 \in \mathcal{R}^{d \times D}$ and $W_2 \in \mathcal{R}^{d \times D}$ may also improve stability.

6 Conclusion

We introduced PKR-QA, a benchmark for procedural knowledge reasoning that challenges models to answer procedural questions. Our evaluation of VLMs revealed their inherent capability to leverage procedural knowledge. However, their closed-loop reasoning mechanisms lack the transparency, controllability, and domain-specific constraints required for mission-critical applications such as medical procedures or industrial automation. To address this gap, we proposed the Knowledge Module Learning (KML) framework, which explicitly grounds reasoning in procedural knowledge graphs and decouples hypothesis generation (via LLM-based program synthesis) from structured execution (via learnable knowledge modules). By constraining reasoning to predefined operations aligned with procedural logic, KML ensures reliability and interpretability without sacrificing performance. Our experiments highlight the promise of

such neurosymbolic architectures, where lightweight, domain-aware modules (trained directly on KG relations) performs well in knowledge-intensive reasoning.

Acknowledgments. This research/project is supported by the National Research Foundation, Singapore, under its NRF Fellowship (Award# NRF-NRFF14-2022-0001). This research is also supported by funding allocation to Basura Fernando by the Agency for Science, Technology and Research (A*STAR) under its SERC Central Research Fund (CRF), as well as its Centre for Frontier AI Research (CFAR).

References

- [1] Ibrahim Abdelaziz, Srinivas Ravishankar, Pavan Kapanipathi, Salim Roukos, and Alexander Gray. A semantic parsing and reasoning-based approach to knowledge base question answering. In *Proceedings of the AAAI conference on artificial intelligence*, volume 35, pages 15985–15987, 2021.
- [2] Jean-Baptiste Alayrac, Jeff Donahue, Pauline Luc, Antoine Miech, Iain Barr, Yana Hasson, Karel Lenc, Arthur Mensch, Katherine Millican, Malcolm Reynolds, et al. Flamingo: a visual language model for few-shot learning. *Advances in neural information processing systems*, 35:23716–23736, 2022.
- [3] Jacob Andreas, Marcus Rohrbach, Trevor Darrell, and Dan Klein. Learning to compose neural networks for question answering. *arXiv preprint arXiv:1601.01705*, 2016.
- [4] Kumar Ashutosh, Santhosh Kumar Ramakrishnan, Triantafyllos Afouras, and Kristen Grauman. Video-mined task graphs for keystep recognition in instructional videos. *Advances in Neural Information Processing Systems*, 36, 2024.
- [5] Shuai Bai, Keqin Chen, Xuejing Liu, Jialin Wang, Wenbin Ge, Sibo Song, Kai Dang, Peng Wang, Shijie Wang, Jun Tang, et al. Qwen2. 5-vl technical report. *arXiv preprint arXiv:2502.13923*, 2025.
- [6] Maciej Besta, Nils Blach, Ales Kubicek, Robert Gerstenberger, Michal Podstawska, Lukas Gianinazzi, Joanna Gajda, Tomasz Lehmann, Hubert Niewiadomski, Piotr Nyczek, et al. Graph of thoughts: Solving elaborate problems with large language models. In *Proceedings of the AAAI Conference on Artificial Intelligence*, volume 38, pages 17682–17690, 2024.
- [7] Antoine Bordes, Nicolas Usunier, Alberto Garcia-Duran, Jason Weston, and Oksana Yakhnenko. Translating embeddings for modeling multi-relational data. *Advances in neural information processing systems*, 26, 2013.
- [8] Chien-Yi Chang, De-An Huang, Danfei Xu, Ehsan Adeli, Li Fei-Fei, and Juan Carlos Niebles. Procedure planning in instructional videos. In *European Conference on Computer Vision*, pages 334–350. Springer, 2020.
- [9] Yingshan Chang, Mridu Narang, Hisami Suzuki, Guihong Cao, Jianfeng Gao, and Yonatan Bisk. Webqa: Multihop and multimodal qa. In *Proceedings of the IEEE/CVF conference on computer vision and pattern recognition*, pages 16495–16504, 2022.
- [10] Wenhui Chen, Zhe Gan, Linjie Li, Yu Cheng, William Wang, and Jingjing Liu. Meta module network for compositional visual reasoning. In *Proceedings of the IEEE/CVF Winter Conference on Applications of Computer Vision*, pages 655–664, 2021.
- [11] Rohan Choudhury, Koichiro Niinuma, Kris M Kitani, and László A Jeni. Video question answering with procedural programs. In *European Conference on Computer Vision*, pages 315–332. Springer, 2024.
- [12] Mark Endo, Joy Hsu, Jiaman Li, and Jiajun Wu. Motion question answering via modular motion programs. In *International Conference on Machine Learning*, pages 9312–9328. PMLR, 2023.
- [13] Nadime Francis, Alastair Green, Paolo Guagliardo, Leonid Libkin, Tobias Lindaaker, Victor Marsault, Stefan Plantikow, Mats Rydberg, Petra Selmer, and Andrés Taylor. Cypher: An evolving query language for property graphs. In *Proceedings of the 2018 international conference on management of data*, pages 1433–1445, 2018.
- [14] Pallabi Ghosh, Nirat Saini, Larry S Davis, and Abhinav Shrivastava. All about knowledge graphs for actions. *arXiv preprint arXiv:2008.12432*, 2020.
- [15] Kaiming He, Xiangyu Zhang, Shaoqing Ren, and Jian Sun. Deep residual learning for image recognition. In *Proceedings of the IEEE conference on computer vision and pattern recognition*, pages 770–778, 2016.
- [16] Lily Hoang, Fiona Liausvia, Yan Liu, and Thanh-Son Nguyen. Semi-automated construction of complex knowledge base question answering dataset using large language model. In *Joint European Conference on Machine Learning and Knowledge Discovery in Databases*, pages 230–248. Springer, 2024.

[17] Edward J Hu, Yelong Shen, Phillip Wallis, Zeyuan Allen-Zhu, Yuanzhi Li, Shean Wang, Lu Wang, and Weizhu Chen. Lora: Low-rank adaptation of large language models. *arXiv preprint arXiv:2106.09685*, 2021.

[18] Drew Hudson and Christopher D Manning. Learning by abstraction: The neural state machine. *Advances in neural information processing systems*, 32, 2019.

[19] Drew A Hudson and Christopher D Manning. Compositional attention networks for machine reasoning. *arXiv preprint arXiv:1803.03067*, 2018.

[20] Aaron Hurst, Adam Lerer, Adam P Goucher, Adam Perelman, Aditya Ramesh, Aidan Clark, AJ Ostrom, Akila Welihinda, Alan Hayes, Alec Radford, et al. Gpt-4o system card. *arXiv preprint arXiv:2410.21276*, 2024.

[21] Shantanu Jaiswal, Debaditya Roy, Basura Fernando, and Cheston Tan. Learning to reason iteratively and parallelly for complex visual reasoning scenarios. *Advances in Neural Information Processing Systems*, 37:137965–137998, 2025.

[22] Justin Johnson, Bharath Hariharan, Laurens Van Der Maaten, Judy Hoffman, Li Fei-Fei, C Lawrence Zitnick, and Ross Girshick. Inferring and executing programs for visual reasoning. In *Proceedings of the IEEE international conference on computer vision*, pages 2989–2998, 2017.

[23] Jie Lei, Licheng Yu, Tamara L Berg, and Mohit Bansal. Tvqa+: Spatio-temporal grounding for video question answering. *arXiv preprint arXiv:1904.11574*, 2019.

[24] KunChang Li, Yinan He, Yi Wang, Yizhuo Li, Wenhai Wang, Ping Luo, Yali Wang, Limin Wang, and Yu Qiao. Videochat: Chat-centric video understanding. *arXiv preprint arXiv:2305.06355*, 2023.

[25] Kunchang Li, Yali Wang, Yinan He, Yizhuo Li, Yi Wang, Yi Liu, Zun Wang, Jilan Xu, Guo Chen, Ping Luo, et al. Mybench: A comprehensive multi-modal video understanding benchmark. In *Proceedings of the IEEE/CVF Conference on Computer Vision and Pattern Recognition*, pages 22195–22206, 2024.

[26] Bill Yuchen Lin, Xinyue Chen, Jamin Chen, and Xiang Ren. Kagnet: Knowledge-aware graph networks for commonsense reasoning. *arXiv preprint arXiv:1909.02151*, 2019.

[27] Ji Lin, Hongxu Yin, Wei Ping, Yao Lu, Pavlo Molchanov, Andrew Tao, Huizi Mao, Jan Kautz, Mohammad Shoeybi, and Song Han. Vila: On pre-training for visual language models, 2023.

[28] I Loshchilov. Decoupled weight decay regularization. *arXiv preprint arXiv:1711.05101*, 2017.

[29] Yue Ma, Yali Wang, Yue Wu, Ziyu Lyu, Siran Chen, Xiu Li, and Yu Qiao. Visual knowledge graph for human action reasoning in videos. In *Proceedings of the 30th ACM International Conference on Multimedia*, pages 4132–4141, 2022.

[30] Muhammad Maaz, Hanoona Rasheed, Salman Khan, and Fahad Shahbaz Khan. Video-chatgpt: Towards detailed video understanding via large vision and language models. *arXiv preprint arXiv:2306.05424*, 2023.

[31] Kenneth Marino, Mohammad Rastegari, Ali Farhadi, and Roozbeh Mottaghi. Ok-vqa: A visual question answering benchmark requiring external knowledge. In *Proceedings of the IEEE/cvf conference on computer vision and pattern recognition*, pages 3195–3204, 2019.

[32] David Mascharka, Philip Tran, Ryan Soklaski, and Arjun Majumdar. Transparency by design: Closing the gap between performance and interpretability in visual reasoning. In *Proceedings of the IEEE conference on computer vision and pattern recognition*, pages 4942–4950, 2018.

[33] Antoine Miech, Jean-Baptiste Alayrac, Lucas Smaira, Ivan Laptev, Josef Sivic, and Andrew Zisserman. End-to-end learning of visual representations from uncurated instructional videos. In *Proceedings of the IEEE/CVF conference on computer vision and pattern recognition*, pages 9879–9889, 2020.

[34] Juhong Min, Shyamal Buch, Arsha Nagrani, Minsu Cho, and Cordelia Schmid. Morevqa: Exploring modular reasoning models for video question answering. In *Proceedings of the IEEE/CVF Conference on Computer Vision and Pattern Recognition*, pages 13235–13245, 2024.

[35] Kumaranage Ravindu Yaras Nagasinghe, Honglu Zhou, Malitha Gunawardhana, Martin Renqiang Min, Daniel Harari, and Muhammad Haris Khan. Why not use your textbook? knowledge-enhanced procedure planning of instructional videos. In *Proceedings of the IEEE/CVF Conference on Computer Vision and Pattern Recognition*, pages 18816–18826, 2024.

[36] Jae Sung Park, Chandra Bhagavatula, Roozbeh Mottaghi, Ali Farhadi, and Yejin Choi. Visualcomet: Reasoning about the dynamic context of a still image. In *Computer Vision–ECCV 2020: 16th European Conference, Glasgow, UK, August 23–28, 2020, Proceedings, Part V 16*, pages 508–524. Springer, 2020.

[37] Jeffrey Pennington, Richard Socher, and Christopher D Manning. Glove: Global vectors for word representation. In *Proceedings of the 2014 conference on empirical methods in natural language processing (EMNLP)*, pages 1532–1543, 2014.

[38] Ethan Perez, Florian Strub, Harm De Vries, Vincent Dumoulin, and Aaron Courville. Film: Visual reasoning with a general conditioning layer. In *Proceedings of the AAAI conference on artificial intelligence*, volume 32, 2018.

[39] Alec Radford, Jong Wook Kim, Chris Hallacy, Aditya Ramesh, Gabriel Goh, Sandhini Agarwal, Girish Sastry, Amanda Askell, Pamela Mishkin, Jack Clark, et al. Learning transferable visual models from natural language supervision. In *International conference on machine learning*, pages 8748–8763. PMLR, 2021.

[40] Nils Reimers and Iryna Gurevych. Sentence-bert: Sentence embeddings using siamese bert-networks. In *Proceedings of the 2019 Conference on Empirical Methods in Natural Language Processing*. Association for Computational Linguistics, 11 2019.

[41] Arka Sadhu, Tanmay Gupta, Mark Yatskar, Ram Nevatia, and Aniruddha Kembhavi. Visual semantic role labeling for video understanding. In *Proceedings of the IEEE/CVF Conference on Computer Vision and Pattern Recognition*, pages 5589–5600, 2021.

[42] Dustin Schwenk, Apoorv Khandelwal, Christopher Clark, Kenneth Marino, and Roozbeh Mottaghi. A-okvqa: A benchmark for visual question answering using world knowledge. In *European conference on computer vision*, pages 146–162. Springer, 2022.

[43] Mili Shah, Joyce Cahoon, Mirco Milletari, Jing Tian, Fotis Psallidas, Andreas Mueller, and Nick Litombe. Improving LLM-based KGQA for multi-hop question answering with implicit reasoning in few-shot examples. In Russa Biswas, Lucie-Aimée Kaffee, Oshin Agarwal, Pasquale Minervini, Sameer Singh, and Gerard de Melo, editors, *Proceedings of the 1st Workshop on Knowledge Graphs and Large Language Models (KaLLM 2024)*, pages 125–135, Bangkok, Thailand, August 2024. Association for Computational Linguistics.

[44] Robyn Speer, Joshua Chin, and Catherine Havasi. Conceptnet 5.5: An open multilingual graph of general knowledge. In *Proceedings of the AAAI conference on artificial intelligence*, volume 31, 2017.

[45] Jiankai Sun, De-An Huang, Bo Lu, Yun-Hui Liu, Bolei Zhou, and Animesh Garg. Plate: Visually-grounded planning with transformers in procedural tasks. *IEEE Robotics and Automation Letters*, 7(2):4924–4930, 2022.

[46] Zhiqing Sun, Zhi-Hong Deng, Jian-Yun Nie, and Jian Tang. Rotate: Knowledge graph embedding by relational rotation in complex space. *arXiv preprint arXiv:1902.10197*, 2019.

[47] Dídac Surís, Sachit Menon, and Carl Vondrick. Vipergrpt: Visual inference via python execution for reasoning. In *Proceedings of the IEEE/CVF International Conference on Computer Vision*, pages 11888–11898, 2023.

[48] Yansong Tang, Dajun Ding, Yongming Rao, Yu Zheng, Danyang Zhang, Lili Zhao, Jiwen Lu, and Jie Zhou. Coin: A large-scale dataset for comprehensive instructional video analysis. In *Proceedings of the IEEE/CVF Conference on Computer Vision and Pattern Recognition*, pages 1207–1216, 2019.

[49] Ng Khar Thoe, Junainah Jamaludin, Yee Jiea Pang, Careemah Choong, Yoon Fah Lay, Eng Tek Ong, Kamalambal Durairaj, Corrienna Abdul Talib, and Chee Keong Chin. Developing conceptual and procedural knowledge/skills of lifelong learners from basic to advance learning: Exemplars, challenges and future direction. *Dinamika Jurnal Ilmiah Pendidikan Dasar*, 14(1):22–35, 2022.

[50] Andong Wang, Bo Wu, Sunli Chen, Zhenfang Chen, Haotian Guan, Wei-Ning Lee, Li Erran Li, and Chuang Gan. Sok-bench: A situated video reasoning benchmark with aligned open-world knowledge. In *Proceedings of the IEEE/CVF Conference on Computer Vision and Pattern Recognition*, pages 13384–13394, 2024.

[51] Xuezhi Wang, Jason Wei, Dale Schuurmans, Quoc Le, Ed Chi, Sharan Narang, Aakanksha Chowdhery, and Denny Zhou. Self-consistency improves chain of thought reasoning in language models. *arXiv preprint arXiv:2203.11171*, 2022.

[52] Zhen Wang, Jianwen Zhang, Jianlin Feng, and Zheng Chen. Knowledge graph embedding by translating on hyperplanes. In *Proceedings of the AAAI conference on artificial intelligence*, volume 28, 2014.

[53] Jason Wei, Xuezhi Wang, Dale Schuurmans, Maarten Bosma, Fei Xia, Ed Chi, Quoc V Le, Denny Zhou, et al. Chain-of-thought prompting elicits reasoning in large language models. *Advances in neural information processing systems*, 35:24824–24837, 2022.

[54] Bo Wu, Shoubin Yu, Zhenfang Chen, Joshua B Tenenbaum, and Chuang Gan. Star: A benchmark for situated reasoning in real-world videos. *arXiv preprint arXiv:2405.09711*, 2024.

[55] Zhiyu Wu, Xiaokang Chen, Zizheng Pan, Xingchao Liu, Wen Liu, Damai Dai, Huazuo Gao, Yiyang Ma, Chengyue Wu, Bingxuan Wang, et al. Deepseek-vl2: Mixture-of-experts vision-language models for advanced multimodal understanding. *arXiv preprint arXiv:2412.10302*, 2024.

[56] Dejing Xu, Zhou Zhao, Jun Xiao, Fei Wu, Hanwang Zhang, Xiangnan He, and Yuetong Zhuang. Video question answering via gradually refined attention over appearance and motion. In *ACM Multimedia*, 2017.

[57] Shuangtao Yang, Mao Teng, Xiaozheng Dong, and Fu Bo. Llm-based sparql generation with selected schema from large scale knowledge base. In *China Conference on Knowledge Graph and Semantic Computing*, pages 304–316. Springer, 2023.

[58] Shunyu Yao, Dian Yu, Jeffrey Zhao, Izhak Shafran, Tom Griffiths, Yuan Cao, and Karthik Narasimhan. Tree of thoughts: Deliberate problem solving with large language models. *Advances in neural information processing systems*, 36:11809–11822, 2023.

[59] Yuan Yao, Tianyu Yu, Ao Zhang, Chongyi Wang, Junbo Cui, Hongji Zhu, Tianchi Cai, Haoyu Li, Weilin Zhao, Zhihui He, et al. Minicpm-v: A gpt-4v level mllm on your phone. *arXiv preprint arXiv:2408.01800*, 2024.

[60] Jiabo Ye, Haiyang Xu, Haowei Liu, Anwen Hu, Ming Yan, Qi Qian, Ji Zhang, Fei Huang, and Jingren Zhou. Implug-owl3: Towards long image-sequence understanding in multi-modal large language models. In *The Thirteenth International Conference on Learning Representations*, 2024.

[61] Shoubin Yu, Jaemin Cho, Prateek Yadav, and Mohit Bansal. Self-chained image-language model for video localization and question answering. *Advances in Neural Information Processing Systems*, 36:76749–76771, 2023.

[62] Zhou Yu, Dejing Xu, Jun Yu, Ting Yu, Zhou Zhao, Yuetong Zhuang, and Dacheng Tao. Activitynet-qa: A dataset for understanding complex web videos via question answering. In *Proceedings of the AAAI Conference on Artificial Intelligence*, volume 33, pages 9127–9134, 2019.

[63] Xiang Yue, Yuansheng Ni, Kai Zhang, Tianyu Zheng, Ruoqi Liu, Ge Zhang, Samuel Stevens, Dongfu Jiang, Weiming Ren, Yuxuan Sun, Cong Wei, Botao Yu, Ruibin Yuan, Renliang Sun, Ming Yin, Boyuan Zheng, Zhenzhu Yang, Yibo Liu, Wenhao Huang, Huan Sun, Yu Su, and Wenhui Chen. Mmmu: A massive multi-discipline multimodal understanding and reasoning benchmark for expert agi. In *Proceedings of CVPR*, 2024.

[64] Yiwu Zhong, Licheng Yu, Yang Bai, Shangwen Li, Xuetong Yan, and Yin Li. Learning procedure-aware video representation from instructional videos and their narrations. In *Proceedings of the IEEE/CVF Conference on Computer Vision and Pattern Recognition*, pages 14825–14835, 2023.

[65] Zijie Zhong, Linqing Zhong, Zhaoze Sun, Qingyun Jin, Zengchang Qin, and Xiaofan Zhang. Synthet2c: Generating synthetic data for fine-tuning large language models on the text2cypher task. *arXiv preprint arXiv:2406.10710*, 2024.

[66] Honglu Zhou, Roberto Martín-Martín, Mubbashir Kapadia, Silvio Savarese, and Juan Carlos Niebles. Procedure-aware pretraining for instructional video understanding. In *Proceedings of the IEEE/CVF Conference on Computer Vision and Pattern Recognition*, pages 10727–10738, 2023.

7 PKR-QA: A Benchmark for Procedural Knowledge Reasoning with Knowledge Module Learning (Supplementary)

In this supplementary, we provide detailed descriptions of the implementation of our proposed method, Knowledge Module Learning (KML), along with the construction of the knowledge graph and the PKR-QA dataset. We also present the detailed breakdown of results for each traversal template for VLMs and NS methods in Table 6 and Table 7.

8 Additional Implementation Details on KML

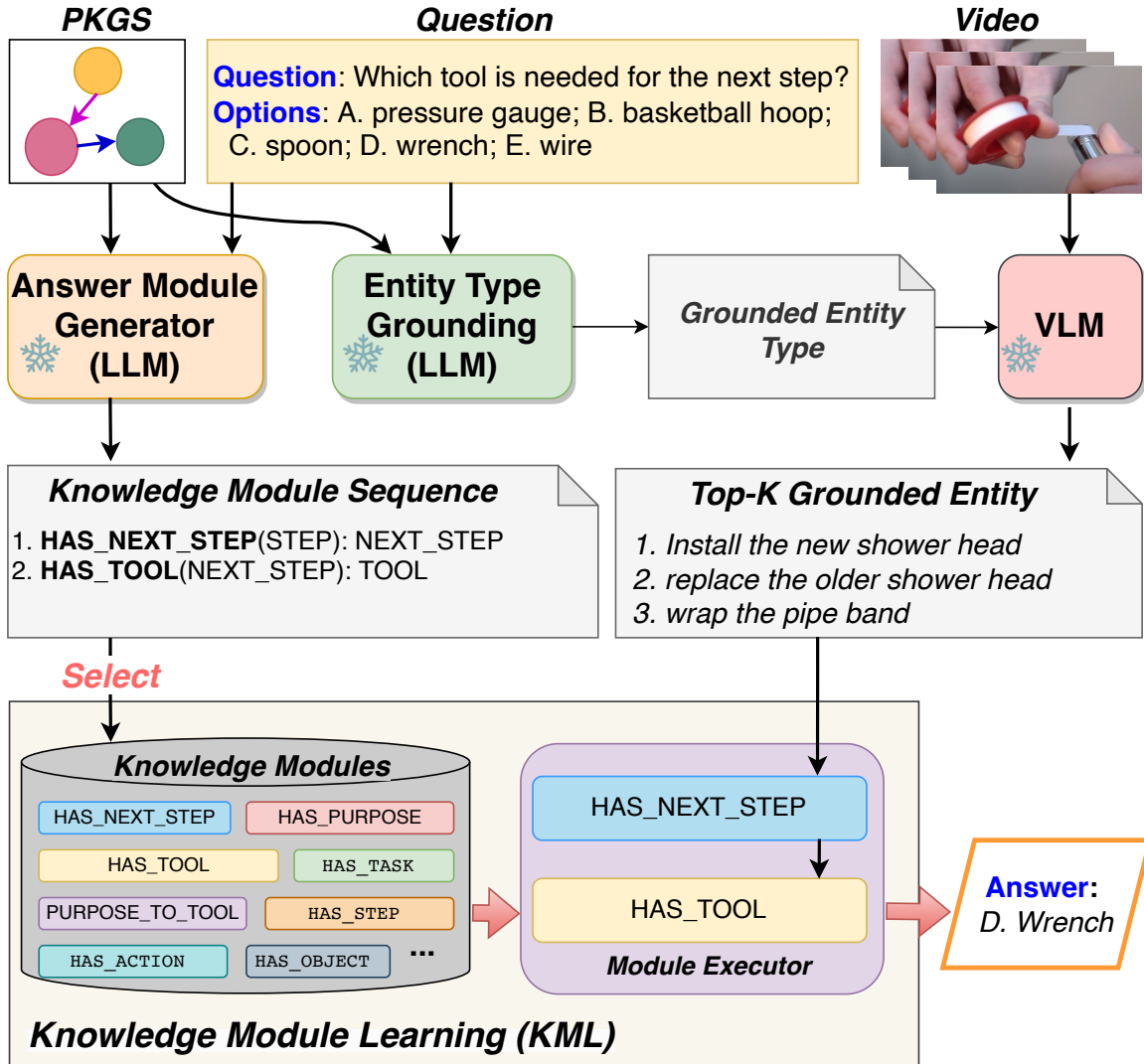


Figure 3: Knowledge Module Learning (KML) for knowledge graph-based procedural video question answering.

Figure 3 shows the overall of our Knowledge Module Learning (KML) framework. Given a video and a question, the framework first identifies the entity type in PKG (e.g. “step”) that should be detected in the video and then recognizes the entity type instances (e.g., step: “wrap the pipe band”) using a VLM. Based on the question and grounded entity type, the *answer module generator* produces the module sequence. Finally, KML executes the sequence of Knowledge Modules to answer the question. In this

example, it first identifies the next step and then determines the tool required for that step, which is a “*wrench*”.

To implement the model Equation (3) and Equation (6) we use LLM with the following prompt.

I have a knowledge graph in the following format.
KG Entities

Step
Action
Object
GroundedTool
Purpose
Domain
Task
START
END
KG Relations

Step → HAS_TOOL → Tool
Tool → HAS_PURPOSE → Purpose
Step → HAS_NEXT_STEP → Step
Domain → HAS_TASK → Task
Task → HAS_STEP → Step
Step → HAS_ACTION → Action
Step → HAS_OBJECT → Object
Purpose → HAS_SIMILAR_PURPOSE → Purpose
Tool → TOOL_TO_STEP → Step
Purpose → PURPOSE_TO_TOOL → Tool
Step → HAS_PREVIOUS_STEP → Step
Task → IN_DOMAIN → Domain
Step → IN_TASK → Task
Action → ACTION_IN_STEP → Step
Object → OBJECT_IN_STEP → Step

I can recognize the step and the task of the video. From knowing the step and the task, I need to answer the question based on the KG relations. I have to traverse from one entity in the KG to the next. The QUESTION is “QUESTION”.

You can answer this step by step. First answer the following question. What should be the first entity I should recognize in the video? Options are only [Step] or [Task].

Then generate the answer, “what is the answer entity for the QUESTION?”

Generate the list of relations that allows you to traverse from the [start entity] to the [answer entity].

Generate a consistent list of relations. Consistent means if Entity_A → KG Relation_X → Entity_B is the k-th relation then the k+1-th relation should start from Entity_B. At every answer check if you can traverse to the current Entity from the start Entity. You should be able to traverse the knowledge graph from start entity to answer entity.

Now generate the answer. You may generate alternative path that allows you to traverse from the start entity to the answer entity in the shortest possible ways also. Generate Python list of relations for each alternative paths.

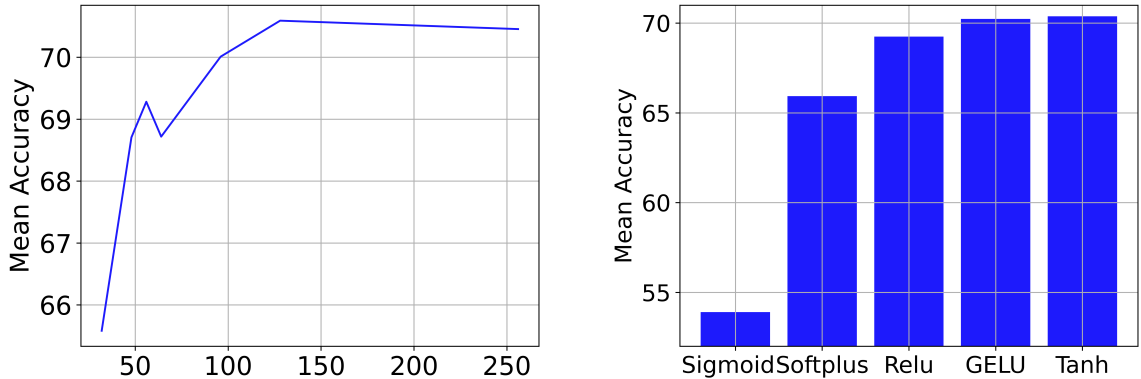


Figure 4: Evaluating the impact of hidden dimension size (left) and the activation function (right) of the Knowledge modules on the validation set.

8.1 Implementation details of KML training

To train KMs we use batch size of 256 triplets with AdamW [28] optimizer (0.01 learning rate), and 100 training epochs. Programs are generated by GPT-4o by default, with other LLMs analyzed. For QA training, KML modules are fine-tuned for 40 additional epochs on video-QA pairs (0.001 learning rate). All KML-F-CLIP models employ 2-layer networks (128 hidden dimensions) with CLIP [39] (ViT-B/32) text embeddings.

8.2 Hyper-Parameter Learning

We evaluate the impact of the hidden size of our knowledge modules. As shown in Figure 4, a small hidden size of 128 is sufficient to learn all modules in the KG, using a total number of 2,107,393 parameters. We also experimented with MSE loss to train the modules, however, the performance was poorer and the combination of contrastive loss and MSE loss did not perform as well as classical contrastive loss. The Tanh activation performs the best among all compared activation functions. The grounding entity E_g of Equation (3) is 100% accurately found by all LLM models.

8.3 Experiments on STAR Benchmark

As before we use CLIP [39] model for entity recognition such as action, relation, object. Specifically, we fine-tune CLIP vision model on the provided annotations of Action Genome dataset and the STAR Benchmark [54] for visual entity recognition using contrastive learning. We design 10 knowledge modules from the hyper-graphs of the training set of the dataset. These are as follows:

- 1. Relation[verb_of_action_class](Entity[action_name])
= Entity[verb_name]
- 2. Relation[object_of_action_class](Entity[action_name])
= Entity[object_name]
- 3. Relation[object_used_by_person_in_relation]
(Entity[relation_name]) = Entity[object_name]
- 4. Relation[relations_by_person_while_executing_action] (Entity[action_name])
= Entity[relation_name]
- 5. Relation[action_class_that_has_verb](Entity[verb_name])
= Entity[action_name]
- 6. Relation[action_class_that_has_object]
(Entity[object_name]) = Entity[action_name]

- 7. Relation[relation_in_which_person_use_object] (Entity[object_name]) = Entity[relation_name]
- 8. Relation[relation_in_which_person_involve_while_executing_action](Entity[relation_name]) = Entity[action_name]
- 9. Relation[action_class_has_next_action_class] (Entity[action_name]) = Entity[action_name]
- 10. Relation[relation_has_next_relation] (Entity[relation_name]) = Entity[relation_name]

These programs are converted to Knowledge-module networks and trained with the hyper-graph data.

Additionally, we use the two utility functions to get the verb, object and relation in the questions and asked LLM to generate the programs.

8.4 KML Programs for PKR-QA

Here we show some of the generated program and the alternative program. To answer the question Q13. What are the additional purposes for which the tool shown in this video can be used, aside from its intended use in the step demonstrated? the following program is generated by GPT-4o.

```

P1
HAS_GROUNDED_TOOL(Step) → GroundedTool
HAS_PURPOSE(GroundedTool) → Purpose
HAS_SIMILAR_PURPOSE(Purpose) → Purpose
P2
HAS_GROUNDED_TOOL(Step) → GroundedTool
HAS_PURPOSE(GroundedTool) → Purpose

```

Similarly, to answer question Q16. What is the other task that use the tool in this video for the same purpose? the following program is generated by GPT4o.

```

P1
HAS_GROUNDED_TOOL(Step) → GroundedTool
HAS_PURPOSE(GroundedTool) → Purpose
IS_SERVED_BY(Purpose) → GroundedTool
USED_IN_STEP(GroundedTool) → Step
IN_TASK(Step) → Task
P2
HAS_GROUNDED_TOOL(Step) → GroundedTool
HAS_PURPOSE(GroundedTool) → Purpose
HAS_SIMILAR_PURPOSE(Purpose) → Purpose
IS_SERVED_BY(Purpose) → GroundedTool
USED_IN_STEP(GroundedTool) → Step
IN_TASK(Step) → Task
IN_DOMAIN(Task) → Domain
HAS_TASK(Domain) → Task
P3
HAS_GROUNDED_TOOL(Step) → GroundedTool
USED_IN_STEP(GroundedTool) → Step
IN_TASK(Step) → Task

```

To answer question 17. What can be the **other task** that use the **object** in this video for the same purpose? the following program is generated by Qwen model.

P1
HAS_OBJECT(Step) → Object
OBJECT_IN_STEP(Object) → Step
HAS_GROUNDED_TOOL(Step) → GroundedTool
HAS_PURPOSE(GroundedTool) → Purpose
HAS_SIMILAR_PURPOSE(Purpose) → Purpose
IS_SERVED_BY(Purpose) → GroundedTool
USED_IN_STEP(GroundedTool) → Step
IN_TASK(Step) → Task

9 Additional Details on Procedural Knowledge Graph

Figure 6 shows PKGS, the schema of our procedural knowledge graph, PKG. PKGS consists of 9 nodes (entities, \mathcal{E}) and 14 edges (relations, \mathcal{R}) connecting these nodes. The nodes represent various types of entities, each capturing a key aspect of procedural knowledge, including:

Domain: contains 12 distinct domains which represent the highest-level category or field under which a set of related tasks are grouped.

Task: represents a specific activity or goal within a domain that requires a set of coordinated steps to complete. Tasks provide the contextual framework for steps, defining the objective that the steps aim to achieve. It bridge the gap between the high-level domain and the detailed procedural steps.

Step: detailing the individual operations necessary to accomplish a specific task. Steps are sequentially organized to capture the logical flow required for successful task completion.

Action: represents atomic operation performed as part of a step. Actions are more granular levels that detail how a step is executed. For example, actions such as “*scrub*”, “*fry*”, or “*pump up*” describe the specific motions or manipulations required in each step.

Tool: represents a specific tool that can be used to assist in performing a step. These tools are not just generic but are tied to the visual evidence in the procedural context. For example, a “*sponge*” and “*cleaning solution*” for the step “*scrub the bathtub*” under task “*clean bathtub*” are tools.

Object: refers to the item being manipulated or acted upon in a step. Objects are central to the procedural actions as they undergo changes or are used as part of the process. Using previous example, in the step “*scrub the bathtub*”, the object is the bathtub.

Purpose: captures the intention or function behind a specific grounded tool within the context of a task and step. It is important for answers the “*what*” tool can be used in the step if we want to achieve a certain task. For example, the “*sponge*” has purpose of “*cleaning*” under step “*scrub the bathtub*”. This node type enhances the knowledge graph’s interpretability by explicitly associating tools with their roles in achieving procedural goals.

START and **END**: two dummy nodes that connect to the starting step and ending step, respectively. These two entities are used to identify starting step and ending step of a task.

The edges in PKGS capture interactions, dependencies, and hierarchies between entities. These relations include:

HAS_TASK: links a **Domain** node to its associated **Task** nodes. It represents the grouping of tasks under a domain.

HAS_STEP: connects a **Task** node to its associated **Step** nodes, capturing the breakdown of the task into actionable units.

HAS_NEXT_STEP: capture the sequential order between **Step** nodes within a task. For example, in the task “*clean bathtub*”, the step “*scrub the bathtub*” is followed by the step “*clean bathtub with water*”. This relation helps in modeling the progression of actions.

HAS_ACTION: connects a **Step** node to its corresponding **Action** nodes, detailing the atomic operations required to execute the step.

HAS_TOOL: links a **Step** node to the **Tool** nodes that assist in performing the step.

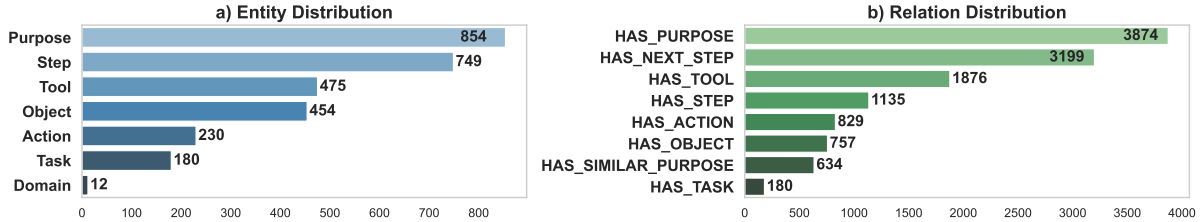


Figure 5: Entity and relation distributions in PKG. The knowledge graph contains a total of 2,954 unique entities and 12,484 relations.

HAS_OBJECT: links a **Step** node to the **Object** nodes that are manipulated or acted upon during the step.

HAS_PURPOSE: connects a **GroundedTool** node to a **Purpose** node, capturing the function or intent of the tool in the procedural context.

HAS_SIMILAR_PURPOSE: links two **Purpose** nodes that share similar intents or functions. For instance, the purposes “*carry liquids*” and “*hold liquids*” are linked with this relation.

The structure of our PKGS not only captures the hierarchical structure and temporal relationships between various components of procedural knowledge extracted from [48], but also extends its expressiveness and utility by incorporating additional layers of information. By enriching the graph with detailed node types and their interconnections, our PKGS provides a more holistic representation of procedural knowledge. As detailed in the main paper, we populate our PKG using annotations from COIN, and additional information from ConceptNet, and data generated and/or grounded using LLMs. The statistic of PKG are presented in Figure 5. Figure 8 shows the entity instances and their relationships for the “make sandwich” task in the procedural knowledge graph

10 Additional Details on the Knowledge Graph and Dataset Construction

Traversal Templates. Table 5 shows 17 traversal templates, together with the sample question, and the number of question-answer instances in the test set.

No.	Traversal Template	Sample Question	Test Size
Q_1	Task $\xrightarrow{\text{HAS_STEP}}$ Step $\xrightarrow{\text{HAS_TOOL}}$ Tool	What tool can be used in this step?	5,024
Q_2	Task $\xrightarrow{\text{HAS_STEP}}$ Step $\xrightarrow{\text{HAS_NEXT_STEP(freq.)}}$ Step	What is the most probable next step?	5,412
Q_3	Task $\xrightarrow{\text{HAS_STEP}}$ Step $\xrightarrow{\text{HAS_NEXT_STEP}}$ Step	What could potentially be the next step?	5,412
Q_4	Step $\xrightarrow{\text{HAS_NEXT_STEP}}$ Step $\xleftarrow{\text{HAS_STEP}}$ Task	What could potentially be the preceding step?	5,408
Q_5	Step $\xrightarrow{\text{HAS_NEXT_STEP(freq.)}}$ Step $\xleftarrow{\text{HAS_STEP}}$ Task	What is the most probable preceding step?	5,408
Q_6	Task $\xrightarrow{\text{HAS_STEP}}$ Step $\xrightarrow{\text{HAS_NEXT_STEP}}$ Step $\xrightarrow{\text{HAS_TOOL}}$ Tool	What tool could be used in the next step?	5,236
Q_7	START $\xrightarrow{\text{HAS_NEXT_STEP(freq.)}}$ Step $\xleftarrow{\text{HAS_STEP}}$ Task	What is the most probable initial step of this task?	1,439
Q_8	Task $\xrightarrow{\text{HAS_STEP}}$ Step $\xrightarrow{\text{HAS_NEXT_STEP(freq.)}}$ END	What is the most probable final step of this task?	1,439
Q_9	Task $\xleftarrow{\text{HAS_TASK}}$ Domain	Which domain does this task belong to?	1,439
Q_{10}	Task $\xrightarrow{\text{HAS_STEP}}$ Step $\xrightarrow{\text{HAS_TOOL}}$ Tool $\xrightarrow{\text{HAS_PURPOSE}}$ Purpose	What is the purpose of the tool used in this step?	2,822
Q_{11}	Task $\xrightarrow{\text{HAS_STEP}}$ Step $\xrightarrow{\text{HAS_ACTION}}$ Action $\xrightarrow{\text{HAS_PURPOSE}}$ Purpose	What is the purpose of the action in this step?	258
Q_{12}	Task $\xrightarrow{\text{HAS_STEP}}$ Step $\xrightarrow{\text{HAS_OBJECT}}$ Object $\xrightarrow{\text{HAS_PURPOSE}}$ Purpose	What is the purpose of the object in this step?	738
Q_{13}	Tool : T_1 $\xrightarrow{\text{HAS_PURPOSE}}$ Purpose: P_1 where Task $\xrightarrow{\text{HAS_STEP}}$ Step $\xrightarrow{\text{HAS_TOOL}}$ Tool : T_1 $\xrightarrow{\text{HAS_PURPOSE}}$ Purpose : P_1	What are the additional purposes for which the tool shown in this video can be used, aside from its intended use in the step demonstrated?	2,611
Q_{14}	Object : O_1 $\xrightarrow{\text{HAS_PURPOSE}}$ Purpose: P_1 where Task $\xrightarrow{\text{HAS_STEP}}$ Step $\xrightarrow{\text{HAS_OBJECT}}$ Object : O_1 $\xrightarrow{\text{HAS_PURPOSE}}$ Purpose : P_1	What are the additional purposes for which the object shown in this video can be used, if I do not want to use it for intended use in the step demonstrated?	674
Q_{15}	Tool : T_1 $\xrightarrow{\text{HAS_PURPOSE}}$ Purpose : P_1 where Task $\xrightarrow{\text{HAS_STEP}}$ Step $\xrightarrow{\text{HAS_TOOL}}$ Tool : T_2 $\xrightarrow{\text{HAS_PURPOSE}}$ Purpose : P_2 $\xrightarrow{\text{HAS_SIMILAR_PURPOSE}}$ Purpose : P_3 and $T_1 \neq T_2$ and $(P_1 = P_2 \text{ or } P_1 = P_3)$	what is an alternative tool that can be used for this step if I don't have the current tool?	875
Q_{16}	Task : A_1 $\xrightarrow{\text{HAS_STEP}}$ Step $\xrightarrow{\text{HAS_TOOL}}$ Tool : T_1 $\xrightarrow{\text{HAS_PURPOSE}}$ Purpose $\xleftarrow{\text{HAS_PURPOSE}}$ Tool : T_1 $\xleftarrow{\text{HAS_TOOL}}$ Step $\xleftarrow{\text{HAS_STEP}}$ Task : A_2 where $A_1 \neq A_2$	What can be other task that can use the tool shown in this video for the same purpose?	2,513
Q_{17}	Task : A_1 $\xrightarrow{\text{HAS_STEP}}$ Step $\xrightarrow{\text{HAS_OBJECT}}$ Object : O_1 $\xrightarrow{\text{HAS_PURPOSE}}$ Purpose $\xleftarrow{\text{HAS_PURPOSE}}$ Object : O_1 $\xleftarrow{\text{HAS_OBJECT}}$ Step $\xleftarrow{\text{HAS_STEP}}$ Task : A_2 where $A_1 \neq A_2$	What can be the other task that use the object in this video for the same purpose?	213
Total			46,921

Table 5: Seventeen traversal templates used to construct question-answer instances in the PKR-QA dataset. For each template, we provide a sample question and the number of test set instances generated. In the traversal templates, **blue text** highlights information grounded in the input video, while **red text** marks the target answer node.

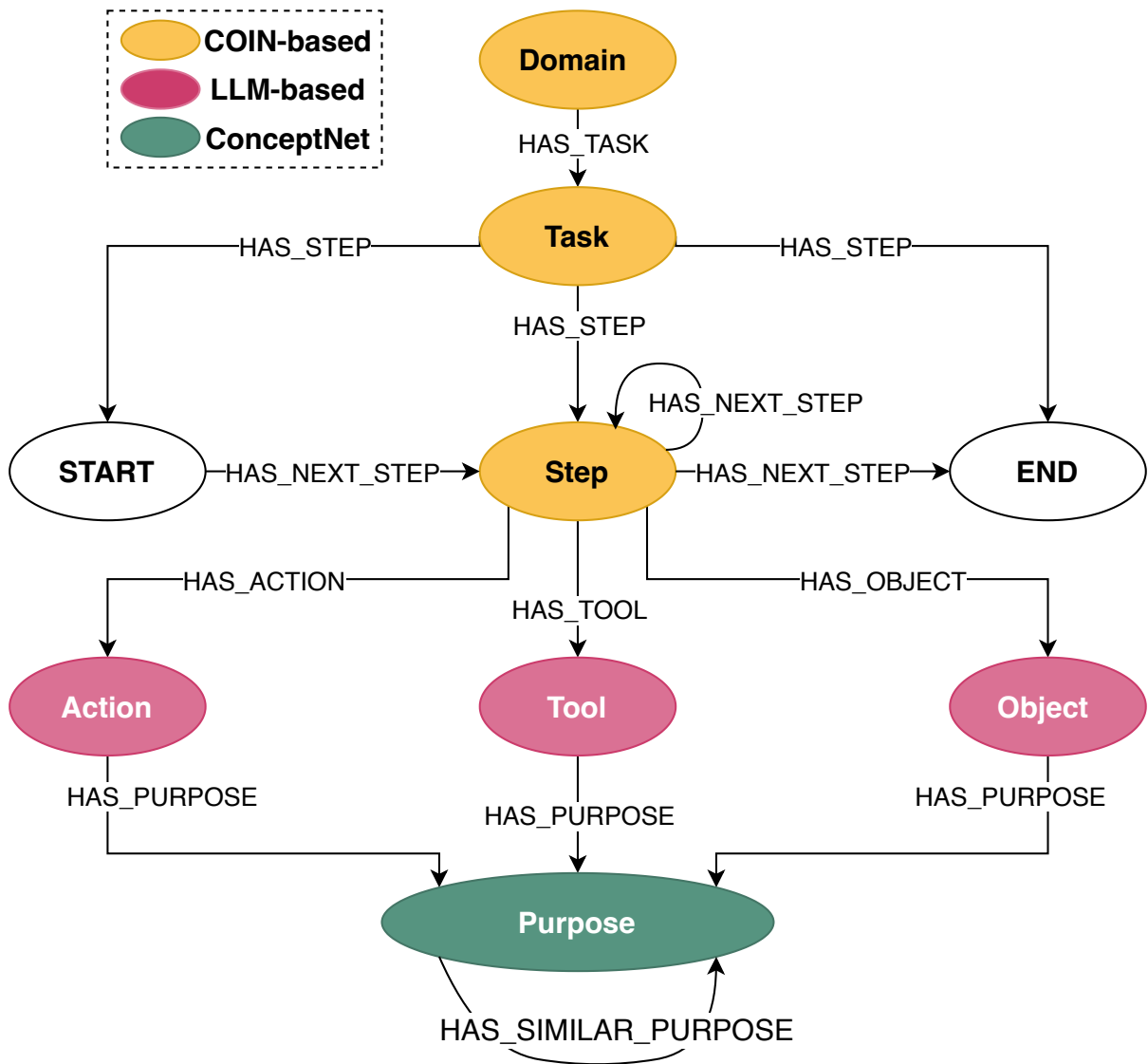


Figure 6: The Procedural Knowledge Graph Schema (PKGS) includes Entities and the potential Relations between them. The instances are populated using annotations from COIN, LLM-generated data, and information from ConceptNet.

10.1 Extract Action and Object from the Annotated Steps

We use GPT-4o from OpenAI³ to extract the action and object based on the text annotation for steps. The prompt is as follows:

You are given a list of steps (each line is a step). For each step, extract the following information if specified:

1. Action: The verb or action being performed.
2. Object: The item or thing on which the action is being performed.

Output as a list of dictionary where each item in the list is the extraction for a step, and each dictionary contains the information extracted for the step. Using this format: [{"Step": "the input step", "action": "", "object": ""}].

Below are example:

Input steps:

clean inner wall of container
place a piece of paper on weighing pan
place weighing sample on weighing pan and read
place the board on each side

Output: [{"Step": "clean inner wall of container", "action": "clean", "object": "inner wall of container"}, {"Step": "place a piece of paper on weighing pan", "action": "place", "object": "piece of paper"}, {"Step": "place weighing sample on weighing pan and read", "action": "place", "object": "weighing sample"}, {"Step": "place the board on each side", "action": "place", "object": "board"}]

Input steps: [Steps]

Output:

10.2 “Purpose” Grounding using GPT-4o

Figure 7 shows the prompt used for *purpose* grounding with GPT-4o. The goal is to ground the purposes of an object, tool, or action in the context of the specific task and step being performed.

10.3 Rephrasing Question Templates

To ensure a diverse range of question phrasings in our dataset, we performed a rephrasing process. Specifically, we prompted GPT-4o-mini to generate up to 30 semantically diverse and contextually appropriate rephrasings for each traversal-based natural language question template. This step leverages the LLM’s capability to enhance linguistic variety while preserving meaning. To ensure quality and consistency, all rephrased questions were manually reviewed to confirm that the original intent was retained. The full prompt used with GPT-4o-mini is shown below:

Rephrase the following question: “[original question sentence]” in 30 different ways while maintaining its semantic meaning and terms such as tool, step, task, domain.

Ensure the rephrasings include a mix of conventional and unconventional sentence structures, such as changing the order of words.

List each variation using * as bullet points.

³<https://openai.com/index/hello-gpt-4o/>

Prompt for Tool

Given a task, step, tool, and a set of options related to the tool's capabilities, your job is to identify and output the relevant options that describe the purpose of using the specified tool in the given step of the task.

Only choose the options that are really relevant. Can output empty list if none relevant options are found. Provide only the relevant options as the output in a list format and rank them from the most relevant to least.

Example:

Task: "CookOmelet"

Step: "pour the egg into the bowl"

Tool: "egg"

Options: ["make breakfast", "hiding at easter", "nurturing", "make omelet", "breed", "cooking", "rolling on white house lawn", "food", "stick to skillet"]

Output: ["make breakfast", "make omelet", "cooking", "food"]

ACTUAL OUTPUT

Task: {task}

Step: {step}

Tool: {term}

Options: {options}

Output:

Figure 7: Prompt template for grounding the *Tool's Purpose*. Similar templates are used for *Object* and *Action*.

10.4 Correct and Incorrect Options Sampling

When generating answer options for each question, relying solely on random sampling can lead to biased options. For instance, frequent terms (e.g., tasks, grounded tools, or objects) are more likely to appear in the correct options compared to infrequent terms, which tend to appear only in the incorrect options. This creates a shortcut for models to identify the correct answer without engaging in true information retrieval and reasoning. To address this issue, we design tailored sampling strategies for each traversal template, ensuring a relative-balanced distribution of terms between correct and incorrect answer options.

Setting	Model	Acc	mAcc	Q_1	Q_2	Q_3	Q_4	Q_5	Q_6	Q_7	Q_8	Q_9	Q_{10}	Q_{11}	Q_{12}	Q_{13}	Q_{14}	Q_{15}	Q_{16}	Q_{17}
Zero-shot	DeepSeek-VL2 (27.4B) [55]	58.4	55.4	69.2	56.7	65.7	64.6	57.2	62.1	61.7	55.9	67.8	54.9	51.6	65.2	25.8	39.9	47.0	45.6	51.6
	MiniCPM-V (8B) [59]	62.6	59.7	73.1	60.1	73.5	71.3	59.7	66.6	60.1	64.3	72.3	61.5	64.3	71.8	20.0	40.2	51.3	51.7	53.1
	mPLUG-Owl3 (7B) [60]	<u>63.1</u>	<u>60.2</u>	71.3	60.1	76.6	73.7	58.7	66.9	65.2	66.0	72.9	62.2	65.5	68.6	19.8	37.7	45.0	52.3	60.6
	Qwen2.5-VL (7B) [5]	59.6	57.8	67.7	57.2	69.5	67.9	57.3	59.4	62.2	62.1	68.9	54.2	58.1	65.2	25.7	46.7	50.2	53.7	56.8
VLM + P.VRL	VideoChat2-HD (7B) [24]	61.2	58.4	72.1	58.5	71.3	70.2	58.5	65.4	60.9	61.4	69.3	58.7	66.3	67.6	18.9	40.2	56.0	49.5	47.4
	DeepSeek-VL2 (27.4B) [55]	64.5	59.9	71.7	64.4	82.5	78.7	63.0	65.7	64.4	65.0	72.3	54.0	63.2	66.0	25.1	42.0	44.5	44.2	51.2
	MiniCPM-V (8B) [59]	67.4	63.8	77.6	64.4	83.7	79.7	63.5	71.5	67.0	69.2	76.3	57.3	67.1	71.4	24.2	50.5	54.6	51.5	55.9
	mPLUG-Owl3 (7B) [60]	65.5	61.6	78.4	59.5	78.5	77.8	60.7	74.4	67.9	71.3	70.3	57.2	67.8	69.9	23.4	46.7	54.5	45.3	43.7
KG-training	Qwen2.5-VL (7B) [5]	<u>69.4</u>	<u>65.8</u>	80.1	66.6	86.2	82.9	65.3	74.4	65.5	67.6	77.1	56.8	72.1	72.1	23.7	51.5	68.5	52.4	55.4
	VideoChat2-HD (7B) [24]	65.5	59.9	74.1	64.9	84.5	82.5	63.7	66.1	66.7	64.9	69.0	54.4	59.3	69.1	23.6	38.7	49.6	42.9	44.1
	MiniCPM-V (8B) [59]	63.5	61.0	74.1	60.0	74.8	70.9	59.1	67.7	63.0	64.1	75.7	58.2	58.5	69.0	25.5	49.6	56.5	55.0	55.9
	mPLUG-Owl3 (7B) [60]	64.8	61.4	75.4	60.2	77.7	75.3	61.2	69.9	65.1	66.4	75.6	57.5	58.1	70.6	24.9	42.6	51.0	53.0	59.2
QA training	Qwen2.5-VL (7B) [5]	<u>67.3</u>	<u>64.1</u>	77.9	62.9	79.8	77.9	65.1	72.4	70.1	69.2	74.0	60.7	68.2	69.7	25.3	47.6	58.4	52.2	57.8
	MiniCPM-V (8B) [59]	71.1	71.4	81.4	64.3	79.6	79.5	63.6	78.0	67.4	71.0	83.6	62.0	77.5	78.2	41.2	63.5	78.9	62.8	81.7
	mPLUG-Owl3 (7B) [60]	71.8	72.4	82.2	64.9	81.2	81.5	63.2	78.4	70.6	70.3	81.9	61.8	80.2	81.7	38.4	66.0	78.4	64.2	85.5
	Qwen2.5-VL (7B) [5]	<u>73.6</u>	<u>73.4</u>	81.3	68.2	83.7	84.9	66.6	78.2	73.3	70.3	85.4	64.0	80.8	78.7	41.2	64.4	76.3	65.9	84.2
KG+QA training	MiniCPM-V(8B) [59]	72.1	72.1	82.4	63.8	81.5	81.9	63.5	79.5	68.6	70.7	84.9	62.7	74.0	80.2	42.5	65.6	77.1	63.6	83.1
	mPLUG-Owl3 (7B) [60]	<u>73.1</u>	<u>73.8</u>	83.8	64.9	83.4	84.3	63.6	80.4	72.8	72.2	84.2	60.9	83.3	82.8	38.9	68.1	78.2	67.0	85.0
	Qwen2.5-VL (7B) [5]	<u>74.2</u>	<u>73.8</u>	83.3	67.3	84.9	85.3	66.4	80.2	73.8	73.0	85.0	64.6	80.9	80.9	41.8	65.7	75.2	66.2	80.5

Table 6: Comparison of VLMs in different settings with detailed scores for each traversal template (Q). Underlined scores denote the best-performing method within each setting, while bold scores highlight the best overall.



Figure 8: Illustration of entity instances and their relationships for the task “make sandwich” within the procedural knowledge graph.

Setting	Model	Acc	mAcc	Q_1	Q_2	Q_3	Q_4	Q_5	Q_6	Q_7	Q_8	Q_9	Q_{10}	Q_{11}	Q_{12}	Q_{13}	Q_{14}	Q_{15}	Q_{16}	Q_{17}
No Training / No Program	ViperGPT GPT-4o + P.VRL	41.6 71.2	40.9 69.0	40.1	50.1	51.8	53.4	34.9	28.8	42.5	45.0	54.8	33.0	46.5	28.2	23.8	32.3	30.9	47.8	50.7
Program Only	IGP (+P.VRL)	62.8	60.0	87.8	52.2	83.4	83.4	50.7	77.0	39.1	50.3	95.1	41.9	81.4	75.9	14.2	62.0	41.3	21.7	62.4
QA training Only	MAC	11.6	20.0	14.10	5.90	4.40	5.70	5.20	14.40	9.80	10.40	74.40	10.20	38.80	21.10	7.70	25.50	27.70	8.00	56.80
KG-training	TransE	63.6	51.6	77.4	65.3	92.1	92.1	64.3	60.7	51.6	53.9	81.8	32.8	40.3	29.9	29.6	31.5	27.2	23.6	22.5
	TransH	73.1	66.3	90.1	63.4	89.6	90.1	63.5	85.3	56.9	54.8	75.8	51.9	50.4	63.6	47.8	59.5	62.2	65.0	56.8
	RotatE	41.6	29.2	23.7	60.3	82.1	81.1	62.5	8.0	19.2	18.6	21.8	13.0	14.0	9.9	11.7	10.2	16.7	20.5	23.0
	TransE+CLIP	56.8	45.4	73.6	59.5	81.7	79.9	58.1	52.9	47.5	47.4	48.3	33.0	27.1	33.3	24.8	36.5	20.2	25.0	22.5
	TransH+CLIP	70.6	65.9	81.0	64.6	85.6	86.2	63.2	78.2	60.8	55.2	80.2	48.9	43.4	67.1	43.9	72.0	54.7	66.4	68.1
	RotatE+CLIP	48.8	35.2	56.8	65.0	88.8	89.7	64.9	4.3	53.6	55.8	54.5	7.0	21.7	7.3	6.6	5.3	6.7	8.0	1.9
	KML-F-CLIP (Ours)	74.6	<u>71.6</u>	91.1	62.3	93.6	93.8	60.8	80.9	61.6	61.9	94.0	58.4	72.1	75.9	37.6	67.5	73.0	65.8	66.2
	KML-Rand (Ours)	73.5	70.0	93.3	59.1	94.7	94.8	59.3	74.1	60.9	59.1	92.7	50.5	76.4	71.3	51.9	73.6	70.7	58.7	49.8
	KML-CLIP (Ours)	75.3	71.4	93.5	58.3	94.8	95.2	58.7	87.4	59.9	63.9	92.6	54.9	67.4	68.7	49.0	72.7	70.6	62.7	64.3
	KML-F-CLIP (Ours)	76.7	75.3	91.1	65.1	93.5	93.8	63.4	83.1	68.7	70.5	94.7	58.2	78.3	74.8	43.7	71.1	80.6	67.8	81.7
KG+QA training	KML-Rand (Ours)	77.4	76.3	93.6	63.5	94.1	94.5	63.8	85.0	68.8	70.0	93.0	54.3	84.9	71.3	50.9	72.0	81.8	69.2	86.4
	KML-CLIP (Ours)	78.1	77.1	93.5	63.7	94.5	94.9	63.3	89.4	72.9	71.8	92.7	53.3	84.5	72.4	51.6	75.1	81.8	69.2	85.4

Table 7: Detailed performance scores of NS methods across traversal template questions. Underlined scores denote the best-performing method within each setting, while bold scores highlight the best overall.

	Question: What tool could be used in the next step? Task: Use Rice-Cooker To Cook Rice Step: Take out some rice.
NEXT_STEP	HAS_TOOL
Output=Next Step	Output=Tool
cook the rice by rice cooker (0.331) put the washed rice into the rice cooker (0.311) soak and wash the rice (0.271) take out some rice (0.154) pour the noodles into the water and stir (0.138)	rice cooker (0.233) water (0.201) bowl (0.197) water container (0.174) water basin (0.167)

Table 8: Step-by-step reasoning of our KML (Knowledge Module Reasoning) method for a given question. The program [NEXT_STEP, HAS_TOOL] is executed by corresponding Knowledge Modules, producing intermediate embeddings with interpretable semantic meaning. This enables explanation of the final output. Experts can modify the program to explore alternative reasoning paths. The program is generated by an LLM based on the question and KG schema.


Question: What could potentially be the next step?
Task: Unclog Sink With Baking Soda
Step: Add hot water to the sink hole.
NEXT_STEP Output=Next Step add baking soda to the sink hole (0.294) add hot water to the sink hole (0.265) add vinegar to the sink hole (0.255) turn on the water tap to wash (0.246) remove the old faucet (0.169)

Table 9: This question demands reasoning over the next step similar to action anticipation. As can be seen the KML method seem to handle the future uncertainties well and list down the plausible set of next steps.

	Question: What is an alternative tool can be used for this step? Task: Make Cocktail Step: pour into the ingredients		
HAS_TOOL Out=Tool cocktail shaker (0.260) cup (0.240) spoon (0.223) jigger (0.220) glass (0.184)	HAS_PURPOSE Out=Purpose measuring liquids (0.359) drinking liquid out of (0.354) cooling liquid by stirring (0.343) drinking out of (0.340) holding liquid (0.340)	SIMILAR_PURPOSE Out=Purpose hold liquids (0.286) hold beverage (0.271) hold liquid (0.261) keep liquids (0.258) holding liquid (0.245)	PURPOSE_TO_TOOL Out=Tool cup (0.339) mug (0.327) measuring cup (0.271) bowl (0.228) glass (0.226)

Table 10: Another example of multi-hop reasoning where the intermediate results are meaningful.